Saccharide Sensing by Affinity Mass Sensors

By

Lee Tin-wan

(李天允)

A Thesis Submitted in Partial Fulfilment

of the Requirements for the Degree of

Master of Philosophy

in

Chemistry

1999

Thesis Committee:

Professor O. W. Lau	(Supervisor)
Professor C. Wu	
Professor Raymund W. M. Kwok	
Professor J. D. R. Thomas	(External Examiner)

Acknowledgements

I would like to express my sincere thanks to my supervisor Prof. Oi-wah Lau for her kind guidance and invaluable advice on my research work. I would also like to thank her for her encouragement throughout the course of my study and during the preparation of this thesis.

I also thank Dr. Bing Shao for his continuous support throughout the course of the research.

Moreover, I am grateful to Miss Alice, Y. M. Chow and Mr. K. W. Wong for their technical support in scanning electron microscopy and X-ray photoelectron spectroscopy respectively. I must also thank my group-mates and friends for their support during these two years.

Finally, I am greatly indebted to my family who support me always.

May, 1999

LEE Tin-wan

Department of Chemistry
The Chinese University of Hong Kong

Abstract

By combining quartz crystal microbalance and boronate affinity chromatography, affinity mass sensors have been fabricated to detect fructose, where 3-aminophenylboronic acid was used as the affinity ligand. For the immobilization of it, two technologies, namely crosslinking method and sol-gel method, have been used in the film preparation. Optimization of immobilization conditions was carried out. Besides, the effects of operation parameters on the response of the sensor were evaluated. Through kinetics analysis, association and dissociation rate constants for this affinity reaction were determined. The sensors were sensitive and reusable since affinity reaction with suitable rate constants was chosen. Calibration graphs for fructose were strictly linear in the range between 0.1 mg/mL and 10 mg/mL. The applicability of the sensors was demonstrated by the determination of fructose in honey samples. Precision, recovery and detection limits were obtained for sensors modified with both methods under optimum conditions.

Comparison was made between sensors fabricated with crosslinking and sol-gel method. The reproducibility of both methods was evaluated by comparing the relative standard deviation of responses from batches of QCMs coated by each method. Their results for fructose determination in honey samples were also examined and proven to have no significant difference between them.

撮要

把石英晶體微天平的概念與硼酸鹽親合色譜的概念相結合，我們制備了親合質量傳感器並以3-氨基苯基硼酸為親合配體，用於檢測果糖。在膜的制備過程中，我們採用兩種方法來固定配體，即交聯法和溶膠-凝膠法。我們對固定化條件進行優化，並評價了各種操作參數對傳感器所產生的信號的影響。通過動力學分析，測定所採用的親合反應的結合速度常數和分離速度常數。由於所選用的親合反應具有合適的速度常數，因此傳感器靈敏並且可重複使用。在 0.1 mg/mL 到 10 mg/mL 的範圍內，果糖的校正曲線呈嚴格的線性。通過對蜂蜜樣品中果糖的實際測定，我們証明了該傳感器可供實際應用 。我們還給出了優化條件下通過兩種固定化方法制備的傳感器的精度、回復率和檢測限。

我們對交聯和溶膠-凝膠法制備的兩種傳感器進行了比較 。通過對兩種方法各自制備的傳感器所產生的信號作出相對標准偏差的比較，我們評價了兩種方法的重現性 。我們也考查了這兩種方法制備的傳感器對蜂蜜樣品中的果糖進行檢測的情況，結果証明沒有顯著區別。

Contents

3. Sol-gel fabrication of affinity mass sensor

Chapter 1

Introduction

1.1 Chemical sensors

A chemical sensor is a device that transforms chemical information, ranging from the concentration of a specific sample component to total composition analysis, into an analytically useful signal [1]. It is typically more versatile and cheaper than traditional instrumentation. Other attractive features such as ease of use, fast and continuous measurement, portability and working *on site* are established.

As an analytical device, a sensor consists of two main parts : a recognition element that is brought into contact with the sample and a transducer. Figure 1.1 describes a design model of a sensor [1, 2]. The recognition process is located in a selective layer or film in close proximity to the transducer. When the analyte interacts with the recognition element, a change in one or more physicochemical parameters associated with the interaction occurs. This change may produce ions, electrons, gases, heat, mass changes, or light, and the transducer converts these parameters into an electrical output signal that can be amplified, processed, and displayed in a suitable form [3]. According to the type of transducer, chemical sensors can be classified as electrochemical sensors, optical sensors, thermal sensors, magnetic sensors and mass or acoustic sensors (Figure 1.2) [1].

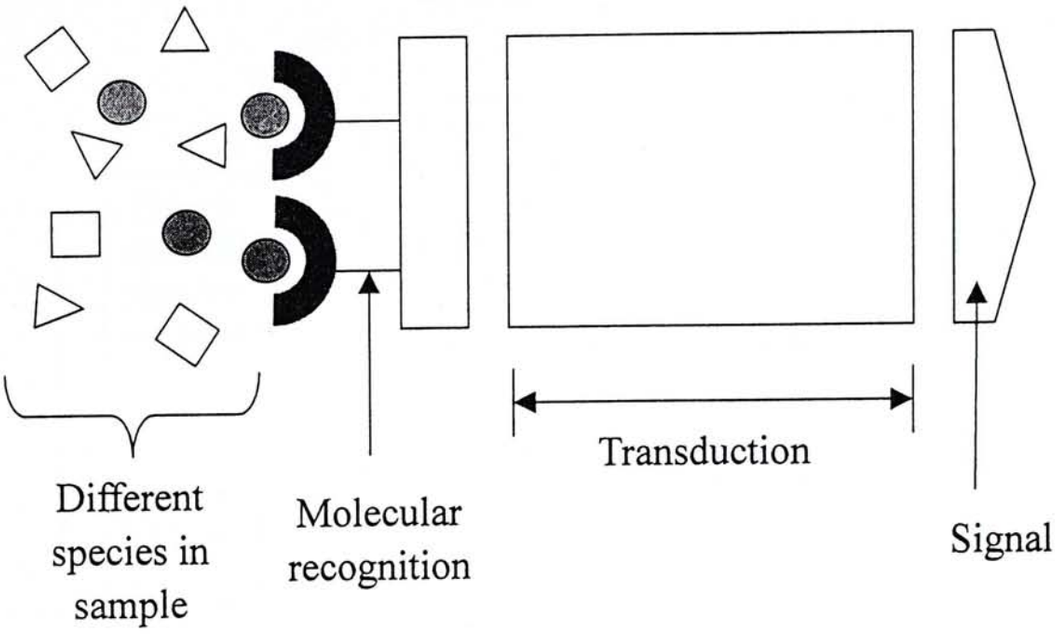

Figure 1.1. Model for chemical sensor. Recognition, transduction and signal generation are coupled.

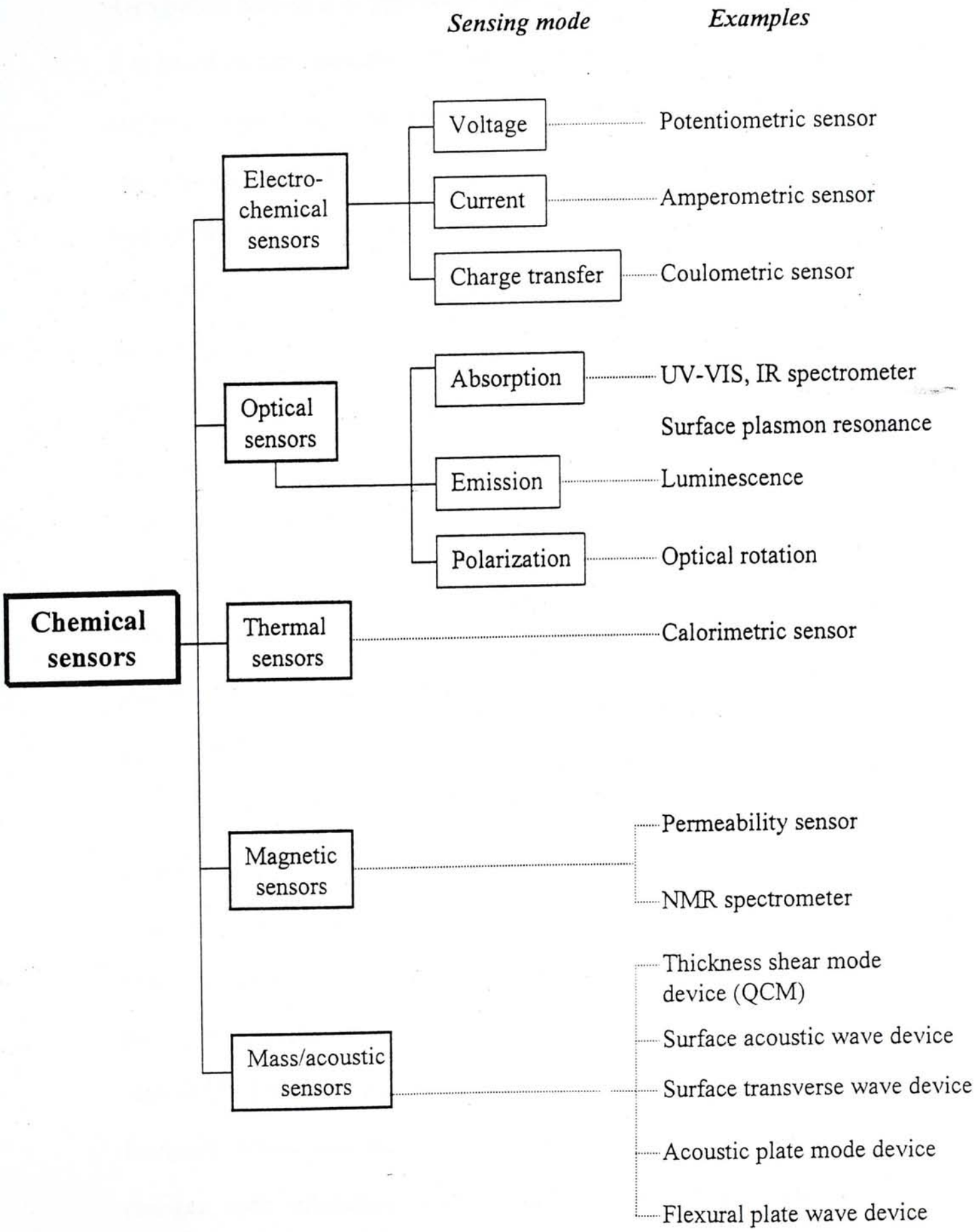

Figure 1.2. Classification of chemical sensors according to the type of transducer.

Recognition process is of paramount significance to the design of a chemical sensor. It is based on the interaction between host molecules or affinity ligands and target analytes, generating host-guest product. Molecular interactions ordinarily encountered in sensing schemes are van der Waals interaction, hydrogen bonding hydrophobic interaction and covalent bonding. The target analyte may be any organic or inorganic or any uncharged molecular species. In order for a sensor to detect an analyte successfully in a complex sample matrix containing some analogously reacting species, high selectivity or specificity is required. To approach this requirement, ligands with appropriate geometry and spatial structure for binding should be constructed.

Biological host molecules such as natural or artificial antibodies and enzymes are promising species to offer either high specificity or an exceptionally high natural selectivity towards their antigens and substrates respectively. Sensors with such biomolecules integrated into the chemical recognition process are known as biosensors, which constitute a subgroup of chemical sensors. However, they have considerably restricted stability and lifetime in many cases [1]. Synthetic ligands are thus derived to mimic biochemical interactions. There are still many different prototype materials which have been chosen as recognition elements for chemical sensors [4], for example polymers with their characteristic inclusion of molecules. Inorganic oxides with their electron, ion, and mixed conduction, show specific changes upon interaction with the molecules to be detected. Organic cage compounds show key-lock incorporation of target molecules.

The first steps towards the development of chemical sensors began by the early 1900s. One of the many landmark achievements in this field was the development of glass electrode for pH measurement by MacInnes [1]. Recently, there has been an overwhelming development in chemical sensors. The (bio)chemical sensors are broadly utilized in medical diagnostics [5-8], the most notable of these are the glucose monitors. Moreover, the sensors gain widespread acceptance in environmental monitoring such as screening waste effluent for the presence of toxic compounds [9-11]. Industrial process control, food and gas analysis can also be achieved by the use of chemical sensors [11-13].

1.2 Quartz Crystal Microbalance

Usually transducers have special demands on the recognition element. For example, in electrochemical sensors, the recognition element should have electrochemical activity. For optical sensors, the optical nature should change accompanying the affinity reaction. In contrast, mass or acoustic transducers have no special demand for the recognition element because mass change must occur with the binding of analytes from the sample to the recognition element which is on the surface of the transducer [14]. Consequently, they have gained more and more interest in chemical sensing in recent years.

Typical acoustic transducers consist of a piezoelectric material with one or more chemically inert metal plate(s) on the surface(s). Piezoelectric crystals are anisotropic

crystals, which were discovered by the Curie brothers in 1880 [15], with no center of symmetry. The piezoelectric effect stated that such crystals give out an electrical signal when mechanically stressed. On the contrary, if an electrical potential is applied, they will oscillate mechanically and this is known as the converse piezoelectric effect. Generally, the amplitude of the oscillation is very small. However, once the frequency of the applied oscillating electrical potential equals a certain frequency, the amplitude increases sharply. This phenomenon is called piezoelectric resonance, and the frequency is known as the resonant frequency of the crystal. Owing to its temperature stability, quartz is the most commonly used piezoelectric material [16, 17]. Other materials such as lithium niobate and zinc oxide may also be good candidates in certain applications.

Through the selection of crystal orientation, the thickness of the piezoelectric material and the geometry of the metal plate, a variety of acoustic wave devices including thickness shear mode (TSM), surface acoustic wave (SAW), flexural plate wave (FPW), acoustic plate mode (APM) and surface transverse wave (STW) devices are designed.

TSM devices constructed on quartz disks are commonly known as quartz crystal microbalances, or QCMs. They are made of AT-cut quartz crystal plates with all unwanted modes of vibration other than TSM sufficiently suppressed . In addition, the resonant frequency of the AT-cut plate is rather insensitive to temperature change in a region around room temperature, and it lies between 5 and 10 MHz typically [17]. The structure of a quartz crystal microbalance is shown in Figure 1.3. It bears a

sandwich structure with two thin layers of gold or platinum on both sides of a thin quartz crystal plate. The electric field, and therefore the vibration of the quartz crystal is essentially confined to the area between the two excitation electrodes. The sensing area is typically 1 cm^2 or less.

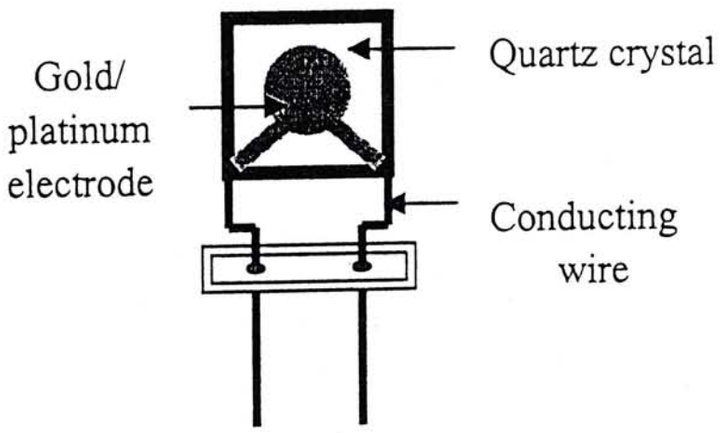

Figure 1.3. A quartz crystal resonator.

Sauerbrey derived an expression relating surface mass changes to shifts in the resonant frequency of quartz crystal in 1959 [14, 18, 19].

$$\frac{\Delta f}{f} = -\frac{\Delta t_q}{t_q} \qquad equ.1.1$$

where f and t_q are the resonant frequency and the thickness of the crystal plate respectively, Δf and Δt_q are the corresponding changes caused by deposited materials. The derivation of the relation relies on the assumption that a deposited foreign material exists entirely at the antinode of the standing wave propagating across the

thickness of the quartz crystal plate, so that the foreign deposit could be regarded as an extension of the plate. If the differences in density and modules constant between the quartz and the deposit are ignored, equ.1-1 can be derived as:

$$\Delta f = -\frac{2f^2\Delta m}{A\sqrt{\rho_q \mu_q}} = -2.3\times10^6 f^2 \Delta m / A \qquad equ.1.2$$

where Δf is the frequency shift in Hz, f is the resonant frequency of the crystal (MHz), Δm (g) is the mass change caused by the deposited materials, ρ_q and μ_q are the density and the modules constants of the quartz crystal plate respectively, and A is the active area of the crystal plate (cm^2). Equ.1.2 suggests that the deposited mass changes can be measured by the corresponding frequency shifts. Since the measurement of the frequency is extremely sensitive, very minute mass changes can be measured. For example, when a 9 MHz quartz crystal plate with 0.2 cm^2 active area is used, about 1 ng of mass change can be measured. The quartz crystal microbalance is thus named due to its excellent mass detection. Typically, QCM measurements are considered accurate provided that the frequency shift of the loaded film being less than 2% of the unloaded frequency. When the loading is larger, the viscoelastisity of the film will affect the frequency measurement, this effect cannot be expressed by the simple Sauerbrey equation, and treatments with other parameters such as impedance introduced should be carried out to allow high mass loading tolerance [15].

Most of the early applications of QCM were conducted in the gas phase. This is because quartz crystals can vibrate with minimal energy dissipation and a stable

oscillation can be obtained in the gas phase. Oberg and Lingensjo [20] made the first contribution to crystal film thickness monitoring with QCM. Warner and Stockbridge were the first to apply QCM on the mass detection of minute substance in vacuum [14]. Over these decades, much effort has been put in QCM as gas sensors. For instance, QCM was used in detection of amine isomers and aromas in 1993 and 1996 respectively [21, 22].

There was a breakthrough in the development of QCM in early 1980s, when several reports appeared in which a quartz crystal microbalance was operated with one face in contact with a liquid. Konash and Bastiaans, Nomura and Okuhara separately studied the behavior of the quartz crystal microbalance in a flow cell [19, 23]. They observed changes in the resonant frequency of the crystal varied with the density and viscosity of the liquids. Later studies found that the morphology and viscoelastisity of the deposited film will also influence on the frequency response. A simple relationship was derived by Kanazawa and Gordon which expressed the change in oscillation frequency of a quartz crystal in contact with a liquid in terms of material parameters of the liquid and the quartz [24]:

$$\Delta f_{\nu} = -f^{3/2}\left(\frac{\rho\eta}{\pi\rho_q\mu_q}\right)^{1/2} \qquad equ.1.3$$

where Δf_{ν} is the frequency shift caused by the properties of the liquid, and ρ and η the density and viscosity of the liquid respectively. This relation had remarkable agreement with experimental results obtained by a test case of water/ethanol solutions.

Prior to the successful operation of QCM in the liquid phase, more attentions are paid to this field. The first work of using QCM as *in situ* mass detector for liquid chromatography was published by Konash and Bastiaans [25]. Stable oscillation at liquid interface and sensitive mass detection have been achieved.

In Schumacher's review [18], the technique of in-situ microweighing with oscillating quartz crystal microbalance immersed in a liquid has proven capable of sensing interfacial process on a microscopic level. This novel approach has also testified its applicability to a variety of surface related processes such as growth/decay of oxidic overlayers on metal electrodes [26]. Furthermore, studies of Langmuir-Blodgett films, self-assembled monolayers, polymer and gel layers with QCMs, have been conducted [27-30]. Recently, a new method for measuring contact angles and surface tension has been derived based on QCM [31].

QCMs have also been extensively applied as biosensors. The first use of bovine serum albumin as coatings on QCM was proposed by Shons *et al.*[32]. Nowadays, QCMs are powerful tools for detection of antigens, antibodies, microorganisms and DNA [33-37].

In addition to the choice of transducer, production of selective layer of chemical sensors is of utmost importance. The affinity ligands for molecular recognition should be immobilized on the surface of the transducers. In this case, film immobilization technologies can be applied to chemical sensor development.

1.3 Film Immobilization Technologies

The combination of chemically or biologically sensitive materials and film formation and immobilization technologies suggest opportunities for development of novel sensors. Parameters of the sensors such as sensitivity, selectivity, stability and reusability strongly depend on the technology and operation conditions chosen. Popular technologies emerged include self-assembly (SA) [38-40]. Self-assembled monolayers (SAM) are molecular assemblies that are formed spontaneously by the immersion of an appropriate substrate into a solution of an active surfactant in an organic solvent. The resulting monolayer film is chemically bonded to the surface, so having high chemical and mechanical stability. This method opens a convenient way to offer a well-ordered film. One of the most promising examples of this approach is the formation of monolayers of organic thiols onto gold surfaces.

The Langmuir-Blodgett (LB) technique offers a better control of creating thin films than SA. It involves transfer of monolayers and multilayers through vertical or horizontal movement from the water-air interface onto a solid substrate. The fabricated film is in a condensed and stable state [41, 42]. Biosensors are a natural application for LB films because a LB bilayer is analogous to a cell wall [43]. Another use for LB films is gas sensing by surface acoustic wave device on which LB film is deposited. However, instrumentation for this technique is expensive and difficult to use.

Plasma polymerization is an advanced method for film formation [44]. When a low

pressure electrical discharge is generated in a gas atmosphere containing organic compounds, polymer film can be deposited on the desired substrate. Form and morphology of the polymer film can be varied by changing the deposition conditions. There have been researches concerning biomolecular attachment onto plasma polymerized surfaces for various applications including glucose sensing and semiconductor immunosensing [45, 46].

Electrochemical polymerization is another tool for preparation of sensitive films [14, 47]. This is usually preformed by oxidation of monomers such as pyrrole, thiophene, or aniline in the presence of an electrolyte in aqueous or organic solutions. The film from *in situ* polymerization process adheres firmly on the substrate. In electrochemical sensors, combined measurements of mass and specific resistance have proved to be suitable for mechanistic studies of interactions between conducting polymers and organic vapors.

Sol-gel method is gradually attracting the attention of the sensor community as a versatile way for preparation of both sensitive and selective film [48]. The terminology "sol-gel" is used to describe processes in which a solid phase is formed through gelation of a colloidal suspension (sol). Alkoxysilanes are used as sol-gel precursor in most cases. They are hydrolyzed with water, and polycondensations follow. Chemically and thermally stable matrices result. Moreover, the matrix has excellent optical transparency and low intrinsic fluorescence. It is evident that the synthesis of gel-glasses doped with chosen molecules is not limited to just a few organics. The flexible solution chemistry and the ability to prepare an essentially

inorganic matrix with little or no heating means that the sol-gel approach is compatible with a wide variety of molecules and can facilitate the recognition step in sensors. The nature of the final film can be regulated by altering the process parameters such as the nature of the catalyst, water and alkoxide content, temperature, ageing and drying time, etc. Current applications of sol-gel technique in sensing include electrochemical sensors of immunoglobulin G and glucose [49-51]. Furthermore, transparent gel matrix has been used in detection of metal ions, in which, the characteristic color changes of the doped gel is monitored [52]. Discrimination among aromas from different wine with the aid of mass sensor has also been reported [22].

1.4 Research Outlines

Our research interest is concentrated on the application of QCM as chemical sensor. Saccharide sensing plays an important role in life science. In the past, it has been achieved by immobilization of enzymes on the surface of the electrode of QCM. However, there are some problems on these sensors as biologically active materials lose their activities easily, especially in hostile environment, resulting in short life of sensors. Besides, due to the strong interaction between enzymes and their substrates in the recognition process, the host-guest products are difficult to be removed retaining the activity of the biological materials. Hence, the sensors cannot be reused, which is an obstacle for both studies in the sensors and commercialization. To overcome drawbacks of natural materials, synthetic ligands are considered.

Affinity chromatography is a protein purification method exploited in biochemistry. It can be applied where any particular ligand interacts specifically with a target molecule. With the marriage of this technique and the concept of quartz crystal microbalance, affinity mass sensor has been established and model for mass sensor has also been set up by Shao [14]. The background of affinity mass sensor will be given in Chapter 2. The first purpose of this work is to validate the concept of affinity mass sensor. A 3-aminophenylboronic acid modified QCM, which responds to D-fructose, is fabricated for this purpose and will also be described in Chapter 2. The effects of various operation parameters on the performance of the sensor will be evaluated. Agreements between the numerical simulation of the affinity mass sensor and experimental results will be shown. The association and dissociation reactions between the affinity ligand and its corresponding ligate are studied with the aid of kinetic analysis proposed by Chaiken *et al.* [53]. The properties of the sensor such as selectivity, stability, and applicability will be also discussed in this chapter.

Chapter 3 reports the use of sol-gel method as an alternative to immobilize affinity ligand on the surface of QCM. The principles of this technique will be reviewed. Factors such as catalyst used, silane to water ratio, ligand loading, temperature, aging and drying involved in optimization of film fabrication will also be discussed. Evaluation of performance of the sensor will be made. This chapter also reports the comparison between sensors derived by covalent-bonding ligand immobilization method described in Chapter 2 and the sol-gel method.

Chapter 2

Saccharide detection by affinity mass sensor

Innovations in the emerging field of piezoelectric devices and advances in using biomolecules in recognition process have been combined to produce biosensors. Unfortunately, these sensors usually suffer from short life due to the ease of losing activity of the biomolecules. Moreover, the low reusability of the sensor cannot be solved easily because the products on specific binding can hardly be washed away. In principle, artificial recognition processes are helpful in overcoming these limitations of biosensors. With replacement of biomolecules using synthetic affinity ligands, revolutionary new sensor, affinity mass sensor, has been established [14]. It is considered as a combination of affinity reaction and the quartz crystal microbalance. The affinity ligands are immobilized on the electrode surface of QCM, and the corresponding ligate can be detected.

In the design of a new affinity mass sensor, an appropriate affinity reaction should be chosen, which depends on the analyte to be determined.

2.1 Concept of affinity mass sensor

2.1.1 Affinity chromatography

Affinity chromatography gives lots of information for affinity reactions useful for the

development of mass sensors. Affinity chromatography was used as far back as 1910 by Starkenstein [see 54, 55], who used insoluble starch as matrix to bind biologically active α–amylase in a specific and reversible manner. With the finding that molecules containing primary amino groups can be coupled on polysaccharide matrices activated by CNBr (Axen *et al.*, 1967) [see 56], an essential prerequisite was created for the development of modern affinity chromatographic procedures and their introduction into laboratory practice.

Affinity chromatography has been qualified for high specific separation, isolation, and purification of native biologically active substances. The basis of the selectivity of affinity chromatography is the use of immobilized biochemicals as the stationary phase [57]. These biochemicals, which are called affinity ligands, can be antibodies, enzyme inhibitors, lectins, or other molecules that reversibly and bioselectively bind to the complementary analyte molecules in the sample, which are known as ligates. The separations exploit the "lock and key" binding that is prevalent in biological systems.

Recently, the terminology of affinity chromatography was further extended by the concept of metal chelate affinity chromatography, charge transfer adsorption chromatography, hydrophobic interaction chromatography, dye-ligand chromatography and covalent chromatography. This stimulated the extensive use of chemiselective affinity ligands such as dyes, boronates, thiol containing affinity sorbents, chelating sorbents (such as IDA and EDTA etc).

In consideration of reusability of the column, the bound ligates should be removed by either specific or nonspecific elution techniques. In specific elution, a free ligand similar or identical to the immobilized affinity ligand, called the inhibitor, compete with the affinity ligand for the binding sites on the analyte. There also exists reversed case, in which the analyte and inhibitor compete for sites on the affinity liagnd. Nonspecific elution involves denaturation of either the ligand or analyte by means of pH, chaotropic agents (e.g., KSCN, urea), organic solvents, or ionic strength. For instance, detergent is promising to disrupt hydrophobic interaction and buffered with high salt concentration detergent can disrupt the ionic interaction.

The continuous deepening of our understanding of affinity chromatography has increasingly provided starting points for the development of affinity mass sensors resting on group-specific interactions and biochemical recognition process.

2.1.2 Basis of affinity mass sensor

In perfect union of affinity chromatography and quartz crystal microbalance, affinity mass sensor [14] was established. The affinity reaction occurring on the surface of the sensor can be described as follows:

$$S + B \longleftrightarrow SB$$

where B represents the affinity ligand, S stands for the corresponding ligate, and SB is the complex resulting from the binding of S and B. When B is immobilized on the surface of the QCM, once the crystal is in contact with a solution containing S, S will

bind to the immobilized B and forms SB, which will also remain on the surface of the QCM. The resonant frequency of the QCM will decrease with the binding of S to B, and the frequency shift is proportional to the concentration of SB. Such a sensor is known as an affinity mass sensor.

In principle, all the affinity ligands used in affinity chromatography can be utilized in affinity mass sensors because the mass changes always occur in an affinity reaction in different phases. Merits of affinity mass sensor over affinity chromatography are the ease in operation and cost effectiveness. Furthermore, the affinity mass sensor can be a powerful tool in the studies of molecular recognition.

Prior to the design of an affinity mass sensor, a model of affinity mass sensor operated in a flow cell has been set up. With numerical simulations [14], the relations between the nature of the affinity reaction and the performance of the sensor have been explored. An affinity reaction with large association rate constant is preferable, so that high sensitivity can be achieved. However, under the same analysis condition, the dissociation rate constant may not favor the reusability of the sensor. In such case, different binding and eluting conditions can be applied so that a reusable sensor with high sensitivity can be derived; however, complicated operation procedures cannot be avoided. For simplicity in operation of the analysis, an alternative is to make a compromise in choosing suitable values of association rate constant and dissociation rate constant of the affinity reaction under the same condition.

2.1.3 Saccharide sensing

Saccharides are nature's conveyors of energy and therefore essential for cell survival. Enormous effort in saccharides analysis was afforded by the use of biologically active molecules, such as lectins, enzymes and even bacteria [55,58-62]. However, such molecules easily undergo degradation. Recently, research interest has been directed towards the saccharide recognition by synthetic ligands. Many known synthetic ligands utilize hydrogen-bonding interactions in order to recognize the corresponding ligates [63-65]. Although the efficiency of such interactions has been well demonstrated in nonaqueous systems, these interactions are less effective in aqueous media when ligates like saccharides are well solvated.

An area that has proved especially useful to the biochemists and has received increasing attention over the past decade is the use of chromatographic materials that contain immobilized boronic acid groups [66]. Ionized boronic acids react readily and under mild conditions with 1,2-diols and 1,3-diols oriented in proper geometry to give five- or six-membered rings. Covalent interactions found in the binding between boronic acids and saccharides in aqueous media are stronger than hydrogen-bonding interactions [67,68]. In a sense, boronates can be considered a "general lectin". Although the specificity for a given saccharide is less than for a true lectin, boronates have several advantages over lectins. First, the boronates are much more stable than the lectins. Second, as a consequence of the greater stability and the varying degree of interaction of boronates with different substances, the limits one must work in to obtain a separation are more flexible. Finally, the low cost of boronates makes sensing with ligands based on them an attractive tool for biochemical investigations.

The affinity reaction between 3-aminophenylboronic acid and D-fructose perfectly demonstrates the applicability of affinity mass sensor. 3-Aminophenylboronic acid was chosen as the affinity ligand because phenylboronic acid has been widely studied for use in liquid chromatography, and derivatives of the phenyl ring provide a convenient means of introducing boronate ligands onto surface of QCM. D-fructose is chosen as the corresponding ligate because it was found to have a high observed association constant to arylboronates in aqueous solutions [66, 69]. Among the saccharides, fructose bears almost the simplest structure which can satisfy the requirements for formation of boronate complexes, and its small size allows it to access the immobilized boronates on the surface of QCM easily. Meanwhile, fructose itself exhibits significance in human health. Fructose is classified as a bulk sweetener. It is completely metabolized by the body and provides an important part of our energy. Hence, fructose, either as the free monosaccharide or as part of the disaccharide, sucrose, is an important source of dietary carbohydrate in most areas of the world. It has been estimated that the average human intake of fructose is of the order of 50-70g per day [70, 71]. As a consequence, analytical methods for the determination of fructose is essential in monitoring the quality of finished products in the food industry.

2.1 Experimental

The affinity reactions usually take place in the liquid phase. In other words, the liquid sample has to be passed over the recognition interface of the sensor. Hence, a flow-

through mode cell has been used to accommodate the QCM. Mass transfer between two phases, with a concurrent chemical reaction is possible in this situation.

2.2.1 Flow-through cell

One of the most valuable assets of flow-through cell is that it allows the sensor operate in continuous configuration [72]. This can serve a variety of functions such as transferring the injected or aspirated sample to the sensor, conditioning the sensor for use, regenerating the sensor between samples and allowing kinetic measurements. In addition, since QCM is extraordinarily sensitive to change in environmental mechanics, using a flow-through cell can avoid unstable oscillation of QCM caused by great changes in the local pressure due to volatilization of the solution contained in a cell with small volume. This is another advantage of flow-through cell over probe-type cell.

When a flow-through cell is used with a reversible sensor, the sample is injected with the aid of a switching valve, and then transported by a carrier (buffer). During the recognition process and mass transfer, the carrier continues to pass through the cell. When these processes ended, the sensor will be regenerated by the carrier stream and ready for the next analysis.

2.2.2 QCA 917 quartz crystal analyzer

As people become more and more interested in sensor applications and tailoring the

chemistry at the surface, quartz crystal microbalances have made their way into the world of chemical analysis. Nowadays, lots of commercial instruments for frequency measurements are available in the market [73]. Among them, Model QCA-917 quartz crystal analyzer is chosen in our study, which can measure both resonant frequency and resonant admittance intensity of a quartz crystal at the same time.

The QCA quartz crystal analyzer (hereafter called the QCA917) is a product of Seiko EG&G. It can measure resonant frequency with an accuracy of 0.1 Hz and at a sample period of 0.1 sec. The resonant admittance intensity can be converted to resonant resistance through calibration. Standard 9MHz, AT-cut quartz crystal microbalance is used in line with this instrument. The oscillation circuit of the QCM is an independent unit such that the QCM can easily be attached and detached. Also, *in-situ* measurement is ensured. The measured data (the resonant frequency and the resonant admittance intensity) are displayed on the main display screen in real time. At the same time, the datum is converted into analog voltage and output to the rear panel. The QCA917 system is provided with an RS-232C interface so that data can be read directly by a computer. Some typical applications of the QCA917 system are summarized in Appendix I [74].

Figure 2.1 depicts the circuit block diagram of the QCA917 system. The oscillator circuit oscillates the quartz crystal at a frequency which is nearly equal to the resonant frequency, which can be obtained by counting the frequency on the frequency counter.

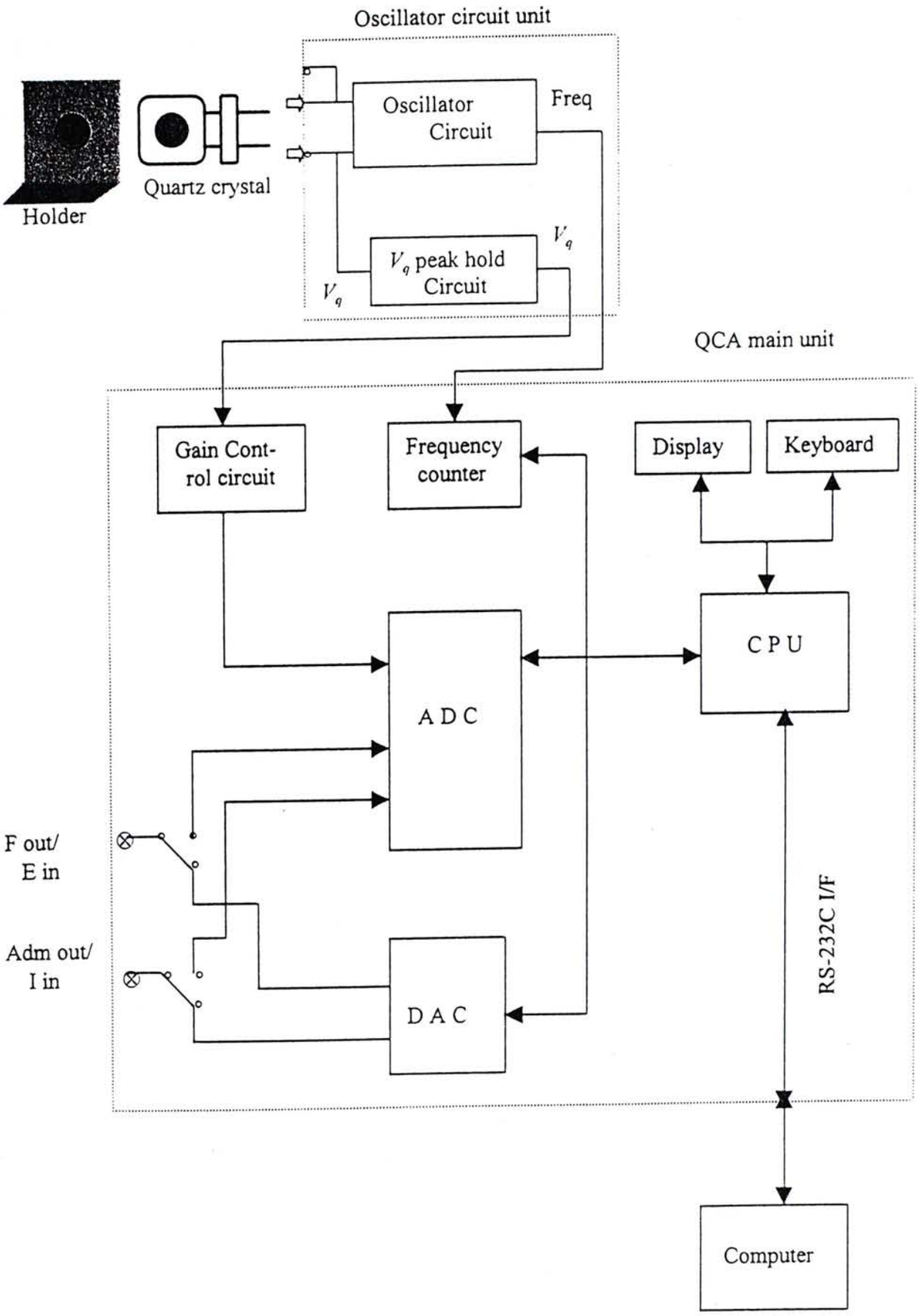

Figure 2.1. QCA917 circuit block diagram.

Another informative datum that can be obtained by the QCA917 system is the resonant admittance. It reflects the viscosity in solution and the viscoelastisity of film. In the case of a film featuring strong viscosity characteristics, a large change in the resonant admittance instead of the resonant frequency occurs. Its measurement principle is shown in Figure 2.2.

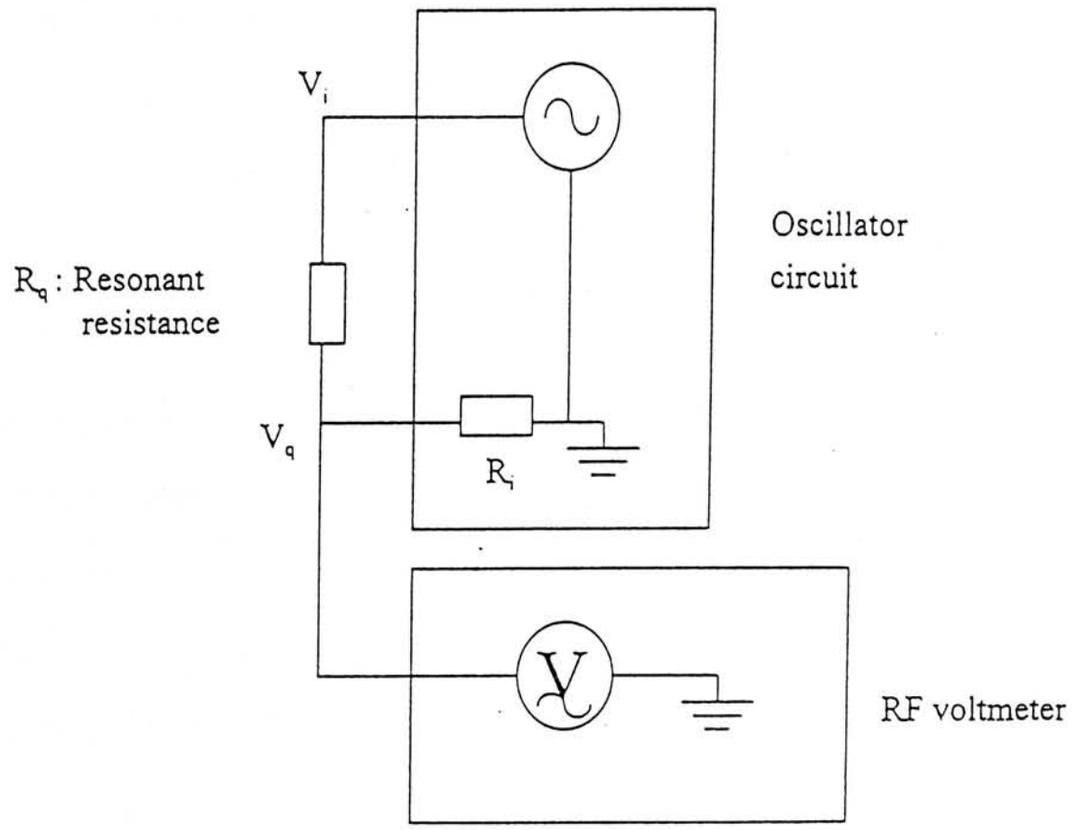

Figure 2.2. Measurement principle of resonant resistance.

In the figure, "R_q" is the resonant resistance of the quartz crystal and "R_i" is the input impedance of the oscillator circuit when the AC signal "V_i" is input to the quartz crystal. The peak voltage of the AC signal "V_q" from the another quartz crystal

terminal can be determined by the following equation:

$$V_q = V_i / (R_q/R_i + 1) \qquad equ.2.1$$

It is then converted into DC voltage, and outputted as the resonant admittance intensity.

The resonant frequency and resonant admittance were recorded *in-situ* by the computer with software written in QBASIC. The programs are shown in Appendix II.

2.2.3 Experimental setup

The experimental setup used was the same as that described by Shao [14]. The schematic diagram for the whole system is shown in Figure 2.3. The QCM was sealed between two O-rings and fixed to a perspex flow-through cell by screws and spacers. The assembly drawing of the flow cell is shown in Figure 2.4. One side of the QCM was in contact with the flowing liquid, and the other side with air. The QCM was easy to be mounted and dismounted. A multi-channel peristaltic pump (ISMATEC IPC-4) and a sample injection valve (Rheodyne Model 5020) were used for transferring liquid. The flow velocity can be adjusted at 100 grades, which can be displayed as 1 to 100. The relations between the grades and the actual flow velocity for aqueous solution corresponding to each grade has been determined and shown in Table 2.1. A linear relation exists between the readout and the flow velocity, and the readout of the grades was used directly to indicate the flow velocities.

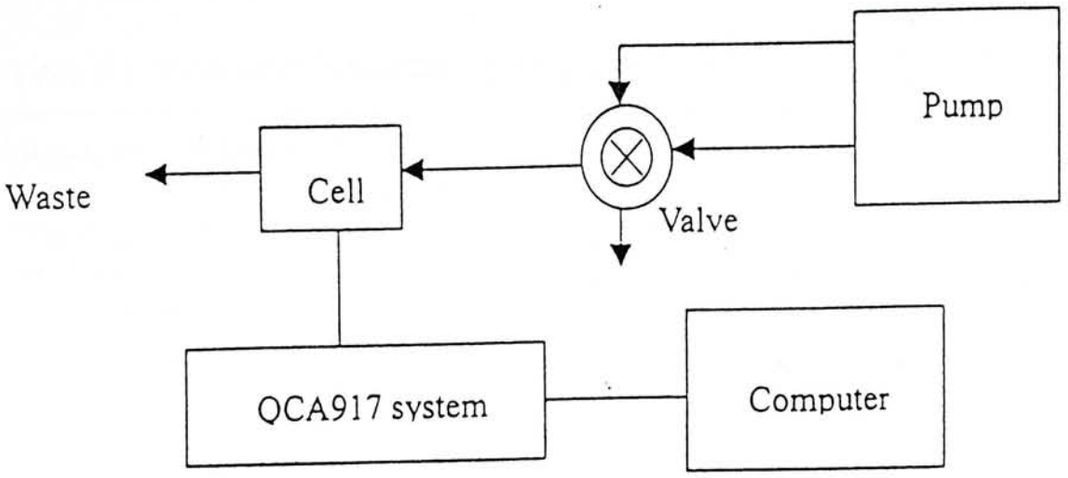

Figure 2.3. Schematic diagram of the flowing system.

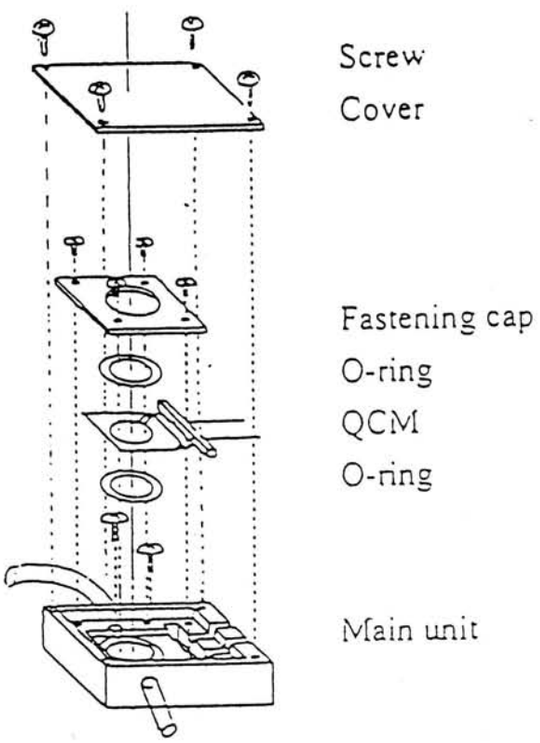

Figure 2.4. Assembly drawing of the flow-through cell.

Table 2.1. Flow velocities corresponding to the readout grades of the peristaltic pump

Readout of grades	2	5	10	20	30	40	50	80	100
Flow velocity (mL/min)	0.12	0.33	0.67	1.31	1.97	2.63	3.26	5.26	6.55

Two channels were used in the peristaltic pump, one for the buffer, and the other for the sample solution. The buffer solution was conveyed to the flow cell through the sample injection valve and in contact with one side of the QCM. The sample solution was delivered to the sample loop of the sample injection valve. Figure 2.5 showed the switching patterns of the valve. Rotation of the knob by 60° switched the valve from one position to another. The two position valves have stops so that they can be turned only back and forth through 60° . The sample volume can be adjusted by the length of the sample loop, it was 0.5 mL unless specified otherwise. When the valve was in the LOAD position, the buffer solution passed from position ② to position ③, while the sample solution passed in the path ⑥→①→④→⑤, filling the sample loop, so that only the buffer solution passed through the flow cell. When the valve was in the INJECT position, the solution would pass in the path ②→①→④→③, and the sample solution in the sample loop would pass the flow cell first, followed by the buffer solution. Hence, a sample pulse would contact one side of the QCM and a response would be obtained. A stable oscillation of the QCM could be obtained using this system with the frequency fluctuations of less than 1 Hz in 30 min.

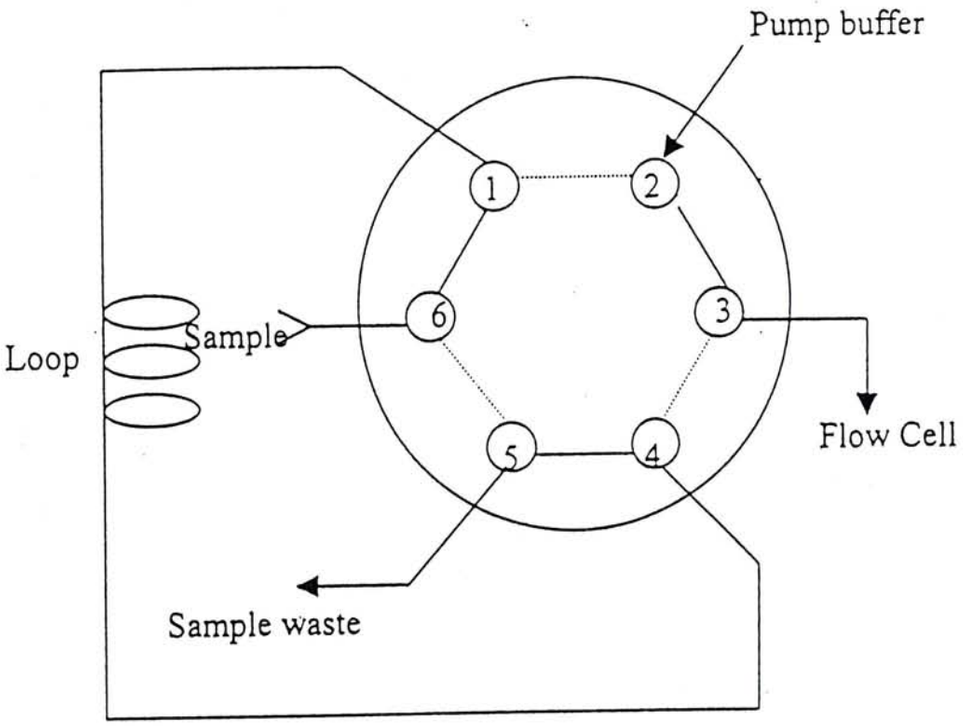

Figure 2.5. Switching patterns of the sample injection valve. The small circles represent the ports in the valve stator. The solid line slots represent the connecting passages in the rotor in the LOAD position. The dotted line slots represent the INJECT position.
(From manual provided by manufacturer)

2.2.4 Sensor fabrication

Polyethyleneimine (PEI) was obtained from Aldrich. Ammonium acetate and D-fructose were from Merck. Glutaraldehyde and 3-aminophenylboronic acid (APBA) were purchased from Acros. D-glucose, sorbital, sucrose and citric acid were obtained from BDH. Ascorbic acid was from Riedel-deHaën. Reagents employed were of analytical grade and solutions were prepared with ultra pure Milli-Q water (Millipore).

A bare QCM was first cleaned with a piranha solution (H_2SO_4 : H_2O_2 = 3:1) [74], followed by exhaustive rinsing with distilled water. *Caution: piranha solution reacts violently with most organic materials and must be handled with extreme care.* The affinity ligand 3-aminophenylboronic acid (APBA) was immobilized on the surface of a QCM as follows: 0.5 μL of 2% polyethyleneimine in ethanol was applied on one side of the gold electrode of the QCM with a micro-syringe. A thin film was formed after drying in air. Then the QCM was dipped in 20% glutaraldehyde aqueous solution. After 2 hours, the QCM was washed with water, dipped into 10 mg/mL 3-aminophenylboronic acid (APBA) solution overnight, and then washed with distilled water, and dried with nitrogen gas. Each step was monitored by the measurement of resonant frequency and admittance. This modified QCM was then mounted in the flow-through cell.

2.2.5 Analysis procedures

For analysis, the sample loop of the sample injection valve was filled with the sample

solution first, and ammonium acetate buffer solution with magnesium chloride added passed through the flow cell, contacting the modified side of the QCM , until a stable baseline was obtained. Then the valve was turned from the LOAD position to the INJECT position, and the sample solution in the sample loop would pass through the flow cell as a plug followed by continuous flow of buffer solution. The resonant frequency and resonant admittance of the QCM were recorded by the computer.

For the determination of association rate constant, solution of analytes at different concentrations were allowed to flow through the flow cell continuously instead of the buffer solution. Whereas for the dissociation rate constant, the analytes bound QCM was flushed using buffer solution without any injection of sample.

2.3 Results and Discussion

2.3.1 Formation of boronate complex

Conventionally, saccharides are analyzed with enzymes, but the enzyme based sensors are unstable in harsh conditions. Frequent replacement for long-term monitoring is unavoidable due to enzyme denaturation. Boronic acid recognition is a remedy. 3-Aminophenylboronic acid (APBA) was employed here to detect D-fructose. APBA is a Lewis acid and it ionizes not by direct deprotonation but by hydration and subsequent ionization to give the tetrahedral boronate anion. Compounds that contain 1,2- or 1,3-diol can react with APBA when the hydroxyl groups are oriented in the proper geometry, leading to the formation of cyclic ester

complex. And hence the reaction is favored in alkaline solution. Figure 2.6 illustrated the hydration of APBA and the affinity reaction occurred between APBA and D-fructose.

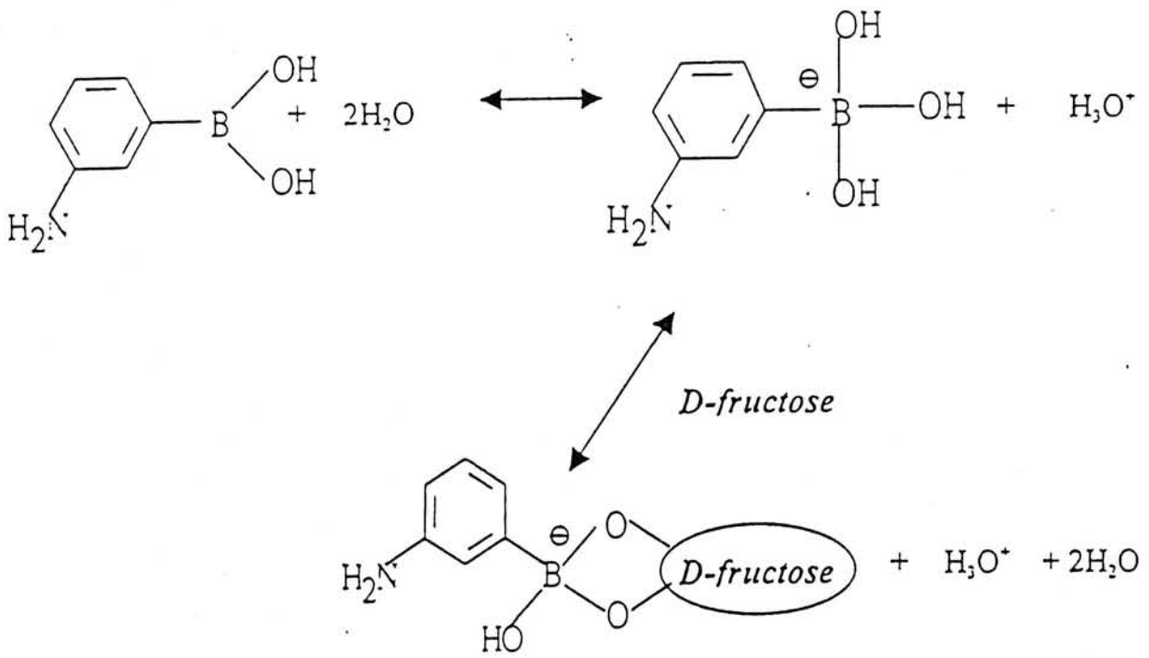

Figure 2.6. Hydration of 3-aminophenylboronic acid (APBA) and the reaction of APBA with D-fructose.

2.3.2 Response curve

In the detection of fructose in aqueous medium by the APBA-modified affinity mass sensor, the frequency was recorded as a function of time and displayed as a response curve, a typical one being shown in Figure 2.7. In this curve, three parameters should be noted, namely the peak response, the response time and the recovering time. Peak response is reflected by the peak height, which is related to the concentration of the analyte. It can be used to evaluate the sensitivity of the sensor. The time corresponding to the peak response is defined as the response time. The recovering

time represents the time at which the response recovers to a position without further change, and theoretically, the response should return to zero. All the aqueous analysis hereafter is based on this kind of curve.

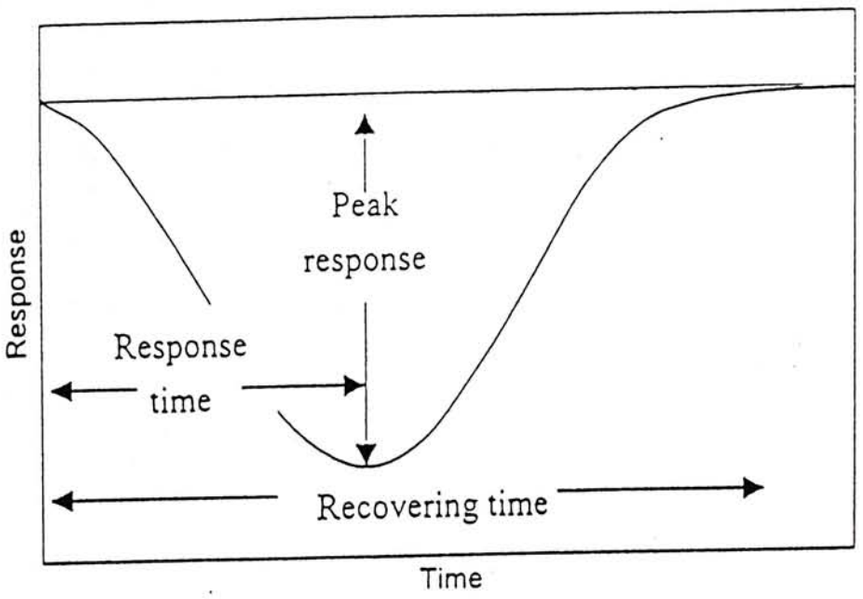

Figure 2.7. A typical response curve.

2.3.3 Ligand (APBA) immobilization

In the development of affinity mass sensor, a coating containing the affinity ligand must be applied on the surface of the quartz crystal microbalance. In this study, crosslinking immobilization method was used. It was based on the formation of covalent bonds between the ligand, by means of bifunctional reagent, leading to three-dimensional, crosslinked ligand aggregates that were insoluble in water. Among the considerable number of crosslinking reagents, glutaraldehyde was by far the most commonly used. It was suggested that the reaction involved conjugate

addition of amino group of the boronic acid to ethylenic double bonds of unsaturated oligomers, contained in the commercial aqueous glutaraldehyde solution.

The resonant frequency and admittance changes for discrete steps in the APBA immobilization were monitored and summarized in Table 2.2. In each step, the observed change in resonant admittance was comparatively much smaller than that in frequency. This could be explained by the fact that when the QCM was coated with a viscoelastic film, the stronger the elastic characteristics, the larger the change in the resonant frequency, and the smaller the change in the resonant admittance. Hence, the frequency drop in each step was an evidence of mass loading.

Table 2.2. Changes during the modification of the QCM

Steps in the modification	Frequency values (Hz)	Resonant Admittance Intensity
Bare electrode	8835479	4490
Modified with polyethyleneimine	8811585 ± 45	4571
Modified with glutaraldehyde	8789532 ± 15	4487
Modified with APBA	8781514 ± 30	4410

In order to obtain highest sensitivity of the sensor, the steps in the ligand immobilization were carefully controlled. Several parameters including solvent, concentration and volume of reagents and immersion duration were studied. Table 2.3 revealed the effects of the concentrations of the crosslinking reagent glutaraldehyde and APBA on peak response. Subsequently, the concentrations of glutaraldehyde and APBA were set to be 20% and 10 mg/mL respectively.

Table 2.3. Effect of concentrations of crosslinking agent glutaraldehyde and affinity ligand APBA on the response of sensor

Concentration of glutaraldehyde (%) [a]	Percentage of maximum response (%)	Concentration of 3-aminophenyl-boronic acid APBA (mg/mL) [b]	Percentage of maximum response (%)
5	84.0	5	66.0
10	88.7	10	100
15	91.7	15	85.3
20	100	20	79.7
25	66.2	25	75.9

[a] Concentrations of APBA used in these 5 trials were 10 mg/mL.

[b] Concentrations of glutaraldehyde used in these 5 trials were at 20%.

Figure 2.8 displayed the response of the APBA modified QCM, under optimized conditions as described in the Experimental section, to fructose. It gave a response of 632 Hz, which was equivalent to a sixty-fold enhancement in response at 5 mg/mL of fructose level when compared to an unmodified QCM.

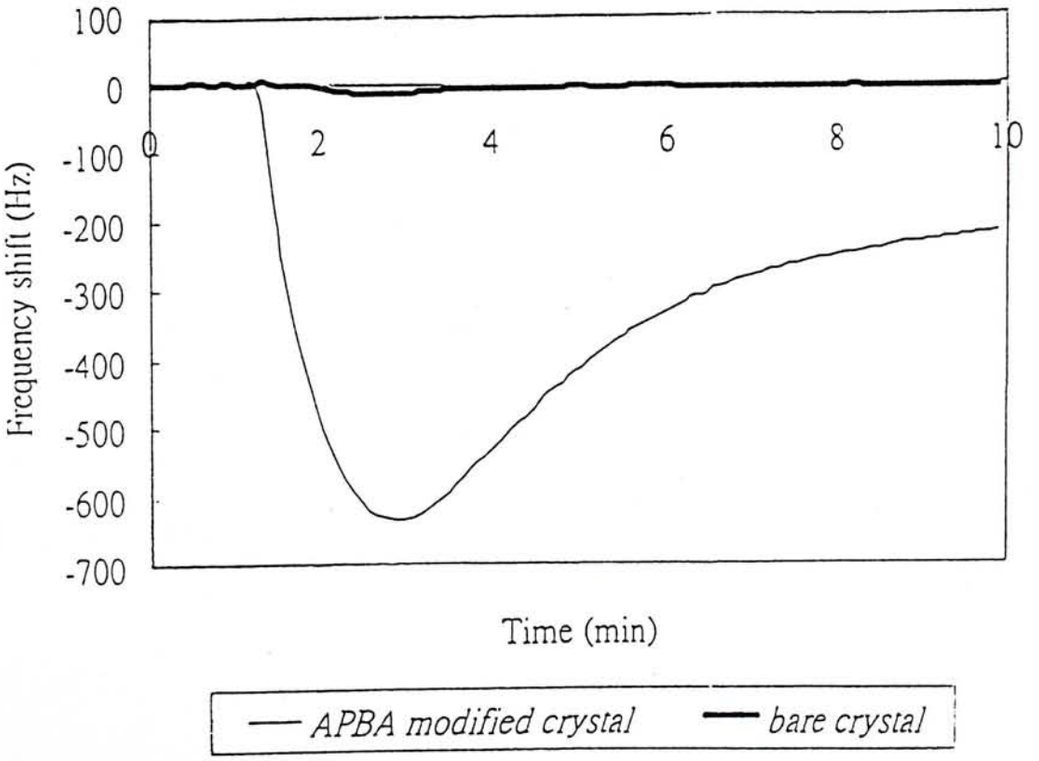

Figure 2.8. Response of APBA modified crystal to fructose (5 mg/mL) at pH 7.9 and flow velocity 10.

Further, it was also noted that the response could not be restored to its original value. This was expected from the numerical simulation [14] of the performance of sensor (see Appendix III) which predicts that the shape of the response curve is mainly governed by the function of $\exp(-k_d t)$, and hence the response can only be restored to a non-zero value known as "near zero" value.

During the reaction, the resonant admittance was also recorded, and only a slight shift of the order 10^1 was observed. This implies that there was little change in the liquid properties before and after the injection of fructose solution, and it coincided with the fact that there was only about 10 Hz decrease in frequency for the unmodified QCM. In this case, the Sauerbrey equation could be applied and a linear relation between the peak response and the concentration of fructose was expected.

2.3.4 Effects of various operating parameters

When choosing conditions for boronate:saccharide complexation, factors that should be taken into consideration included the pH of the buffer and its ionic strength. Since anionic form of the dihydroxyboryl group would favor the affinity reaction, the response of the APBA modified sensor was examined as a function of pH in the range of 7 to 9.5. As shown in Figure 2.9, the sensor showed maximum response at pH 7.9, and hence 7.9 was taken as the optimum pH.

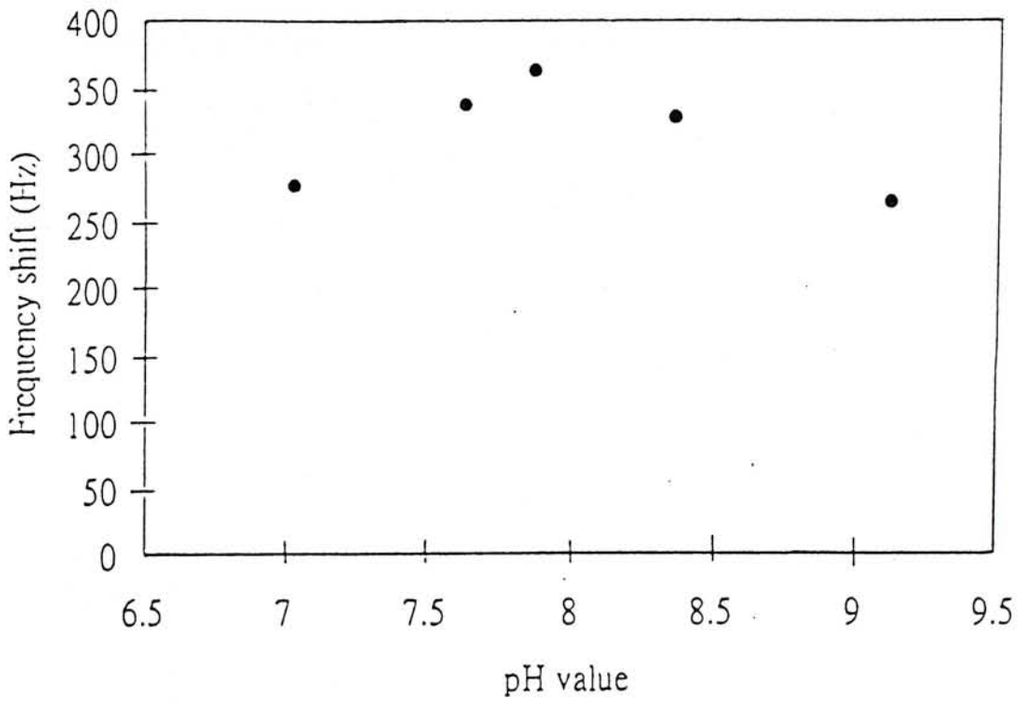

Figure 2.9. Effect of pH on the peak response for fructose (3 mg/mL) at flow velocity 10.

Table 2.4 showed the effect of variation in the salt concentration on the sensing of fructose with the APBA modified sensor. The change in response caused by a change in salt concentration could be accounted for by considering the ionization of boronic acid. An increase in the ionic strength of the buffer decreased the pK_a of the ionization, due to the shielding of the charges on the surface of the sensor. Hence, at a fixed pH, an increase in salt concentration increased the concentration of boronate anions with a resulting increase in response. The use of a divalent cation (Mg^{2+}) in the buffer was more efficient in shielding the charges. This was evidenced by the observation that the response using 0.2 M ammonium buffer solution with 0.1 M $MgCl_2$ added was about 1.5 times of that with 1 M NaCl added.

Table 2.4. Effect of varying the salt concentration on the response of sensor to 5 mg/mL fructose solution

Buffer solution applied	Response (Hz)
0.2 M NH_4Ac	360
0.2 M NH_4Ac + 1 M NaCl	414
0.2 M NH_4Ac + 0.1 M $MgCl_2$	632

The influence of sample volume V_s on peak response was shown in Figure 2.10. The larger volume induced a larger peak response, however, both the response time and the recovering time were prolonged. This coincided with the prediction of the numerical simulation [14].

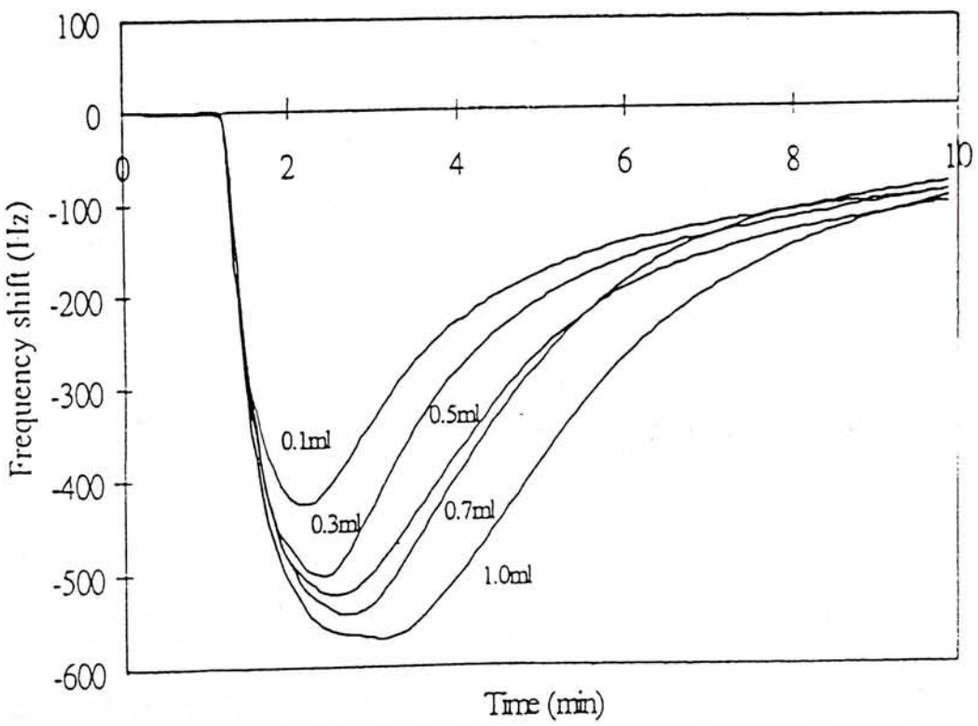

Figure 2.10. Effect of the sample volume on the response curve for fructose (4 mg/mL) at pH 7.9.

The flow velocity of buffer and sample also affected the peak response. Maximum response was obtained at the lowest flow rate. There was an obvious decay in response accompanying the increase of flow rate as shown in Figure 2.11, which was also in agreement with the prediction of numerical simulation [14]. As a consequence, the choice of sample volume and flow rate involved a compromise between sensitivity and response time of the sensor.

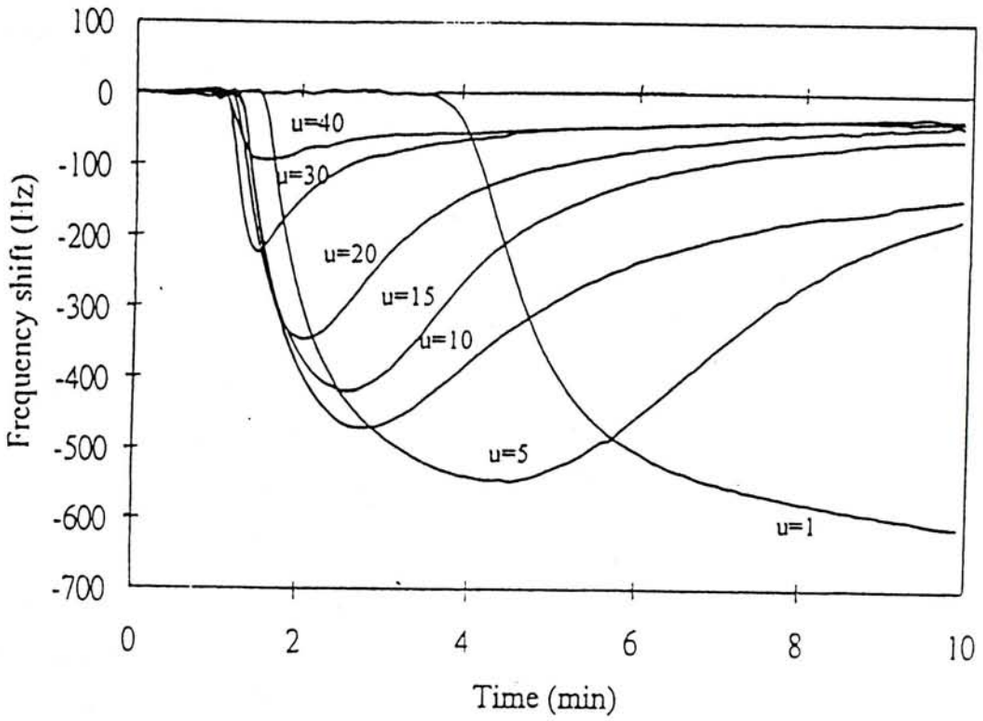

Figure 2.11. Effect of the flow velocity on the response curve for fructose (5 mg/mL) at pH 7.9.

2.3.5 Calibration and Reproducibility

The APBA modified sensor showed a linear relation between peak response and fructose concentration. Figure 2.12 shows a typical calibration graph over the range of 0.1 mg/mL to 12 mg/mL and the correlation coefficient was found to be 0.999. The lower limit for reliable detection (LRD), which represented frequency change

three times larger than the noise observed, was determined to be 3 Hz. The relative standard deviation for 10 replicate injections was 1.5% at 5 mg/mL fructose level.

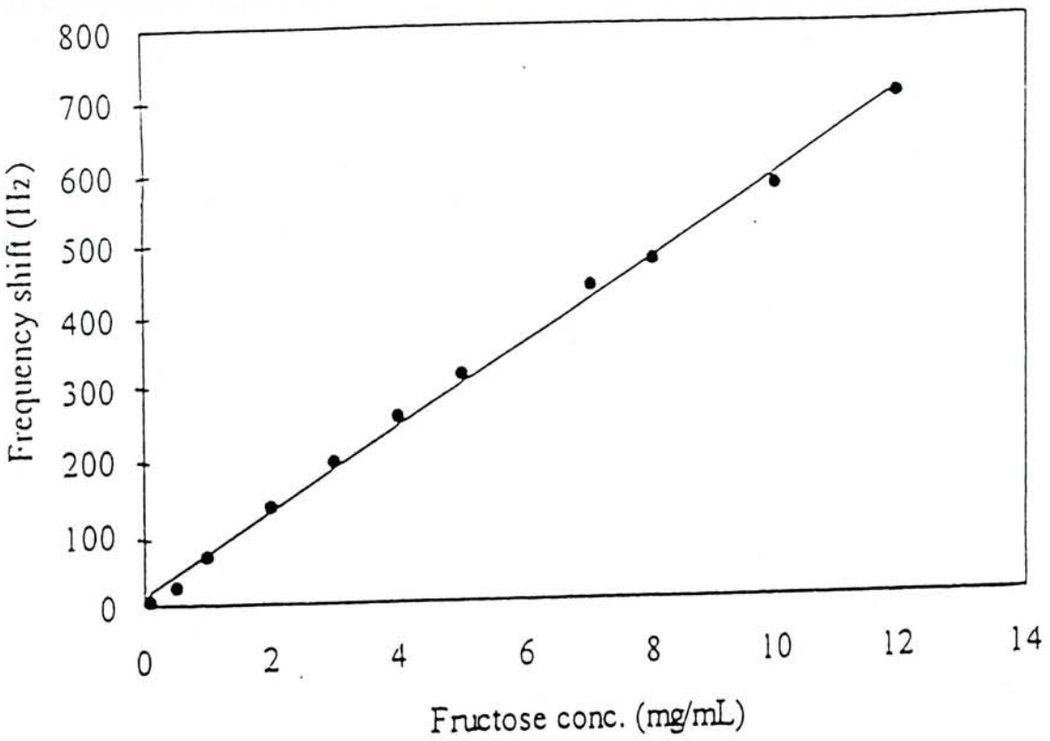

Figure 2.12. Response of APBA modified crystal to fructose solutions with different concentrations.
(flow rate = 10 and sample volume = 0.5 mL)

2.3.6 Kinetic Analysis

The values of the association rate constant (k_a) and the dissociation rate constant (k_d) of the affinity reaction between 3-aminophenylboronic acid and fructose had been determined using the method of Kinetic Analysis proposed by Chaiken *et al* [see 14, 53].

For the determination of k_a, solutions of fructose at different concentrations were allowed to flow through the flow cell separately to replace the buffer solution and the curves of the frequency values vs. time were recorded for a certain time interval for

each fructose concentration. These were known as association curves and a typical one is shown in Figure 2.13.

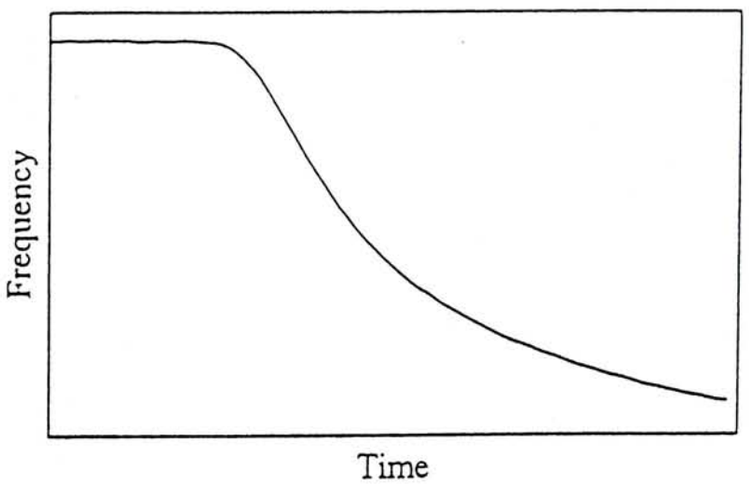

Figure 2.13. The association curve of APBA modified crystal to the continuous solutions of fructose.

Because the Sauerbrey equation can be applied in this analysis, the following equations can be deduced [53]:

$$\frac{df_k}{dt} = \frac{f_{k+1} - f_{k-1}}{t_{k+1} - t_{k-1}} \qquad equ.\ 2.2$$

$$\frac{df}{dt} = A - (k_s) \times f \qquad equ.\ 2.3$$

$$k_s = k_a C_s + k_d \qquad equ.\ 2.4$$

For each association curve, the slope at each frequency f, $\frac{df}{dt}$, was calculated using *equ.*2.2 and plotted against f; the linear part of this plot (see Figure 2.14) can be

described by *equ*.2.3, and the slope k_s can be deduced for each fructose concentration C_s. From *equ*.2.4, k_s was a linear function of C_s, and k_a was the slope of the plot of k_s vs C_s (see Figure 2.15) and was calculated to be $25.2 M^{-1} s^{-1}$.

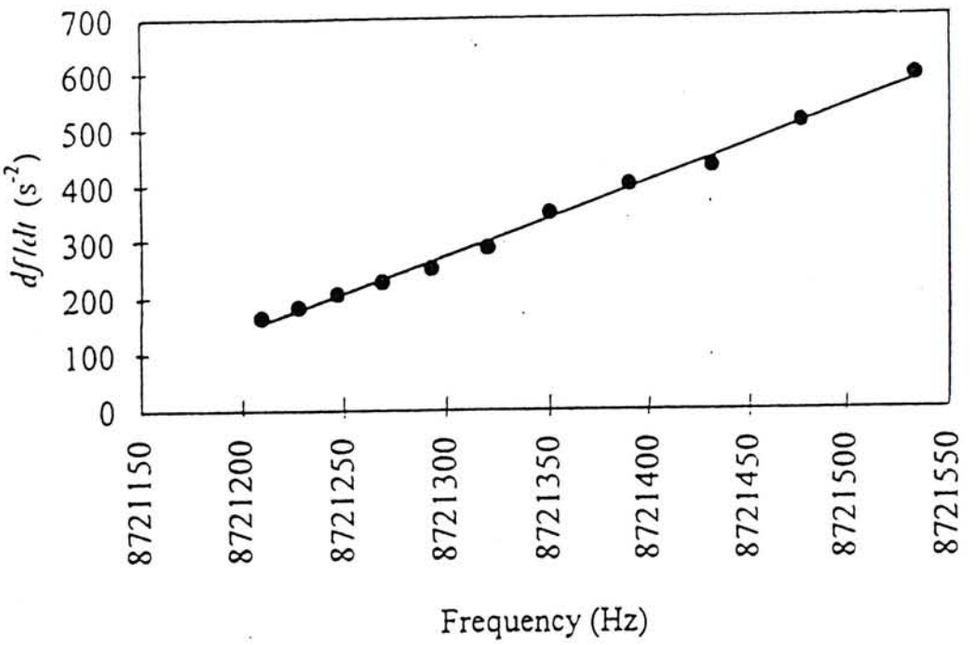

Figure 2.14. The plot of *df/dt* vs frequency.

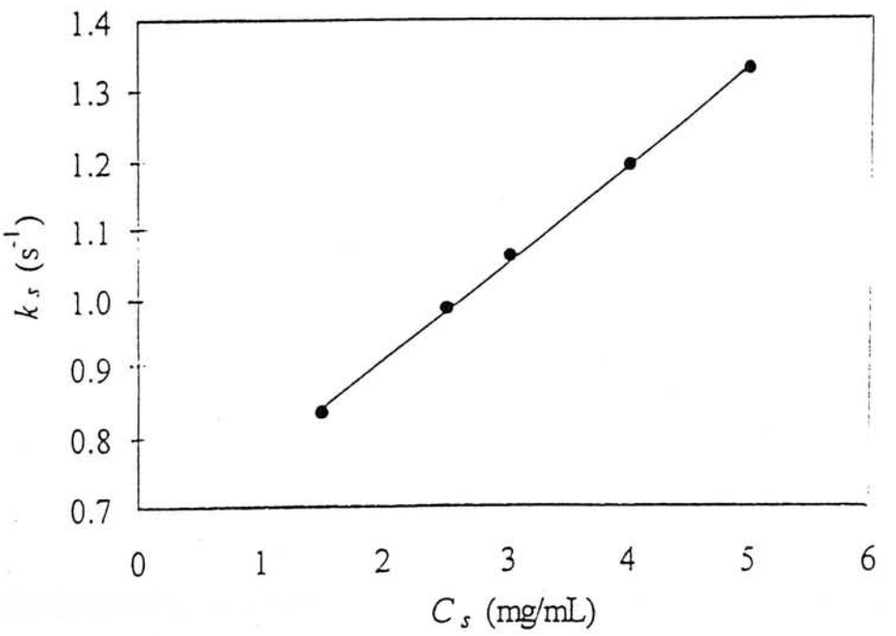

Figure 2.15. The plot of k_s vs C_s.

For the determination of k_d, the fructose-binding sensor was washed using the buffer, and the curves of frequency vs. time were recorded, which are called dissociation curves (see Figure 2.16).

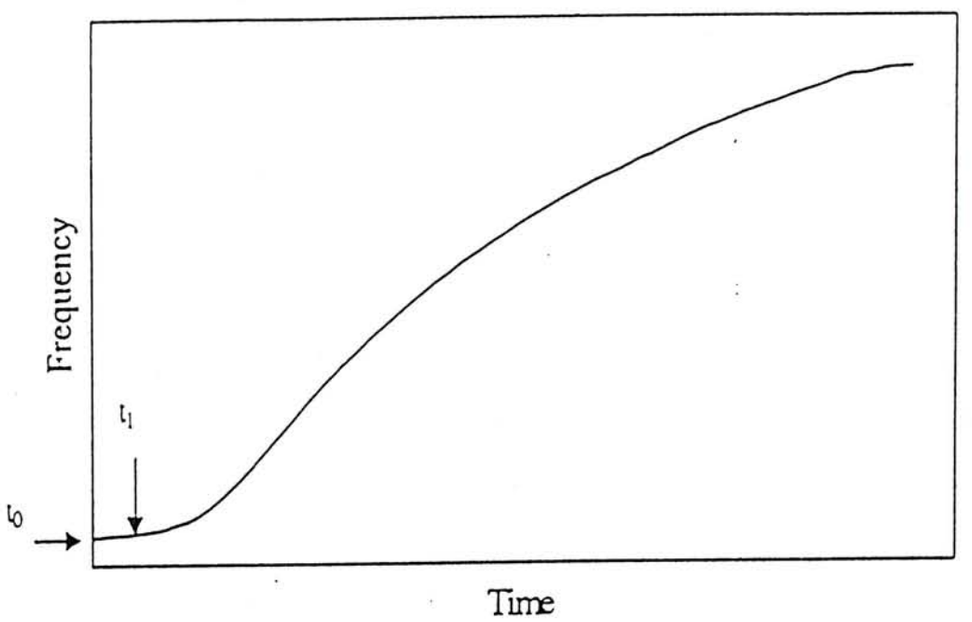

Figure 2.16. The dissociation curve of APBA modified crystal (bound with a 5 mg/mL fructose solution) washed by pH 7.9 buffer.

The original equation in Reference 53 can be modified as

$$ln\left[\frac{f_n - f_0}{f_1 - f_0}\right] = k_d(t_n - t_1) \qquad equ.\ 2.5$$

where f_n is the frequency value along the dissociation curve, f_1 the frequency value where the dissociation started at t_1, and f_0 was the frequency value of the fructose-

binding sensor just before the fructose was washed off at t_0. Figure 2.17 was the corresponding plot using only the data in the linear part of the dissociation curve and from *equ*.2.5, k_d is the slope of this plot. The calculated values of k_d are shown in Table 2.5, with an average value of 0.75 s^{-1}. Practically, the peak response of the sensor restored to the "near zero" value within 10 min., suggesting the sensor to be reusable.

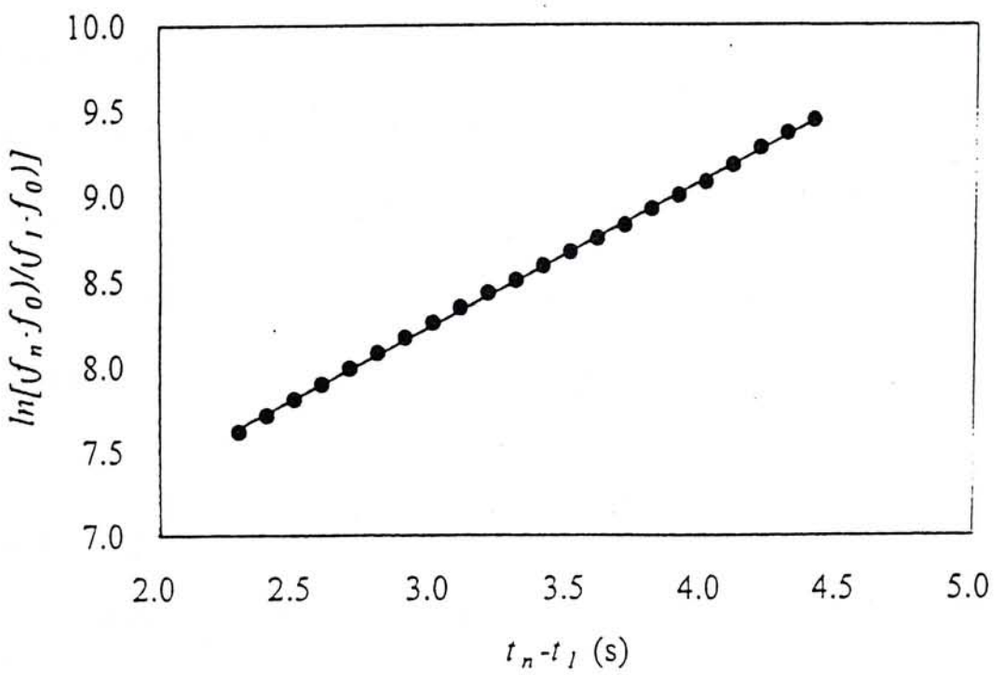

Figure 2.17. The plot of $ln[(f_n-f_0)/(f_1-f_0)]$ vs (t_n-t_1) at 5 mg/mL fructose.

Table 2.5. Values of dissociation rate constant, k_d, at different fructose concentrations

Concentration of fructose (mg/mL)	0.5	0.8	1.5	2.0	2.5	3.0	4.0	average
k_d (s^{-1})	0.771	0.761	0.754	0.713	0.724	0.733	0.798	0.75

2.3.7 Stability of sensor

The operational stability of the sensor was studied over a period of 7 days and for about 8 hours of continuous operation per day. After the first 4 days, a decay of less than 5% of the initial response was observed and the response gradually decreased to 80% of the original level at the end of the 7^{th} day.

2.3.8 Determination of fructose in real samples

Monosaccharides other than fructose and oligosaccharides show lower affinity to APBA, but still may cause interferences. The effects of some common ingredients in juices on the determination of fructose were studied. The results using a synthetic apple juice sample [76] are tabulated in Table 2.6. It can be seen that these ingredients did not interfere with the determination at the levels commonly found in real samples.

The accuracy of the sensing using APBA modified QCM was assessed by determining fructose in a synthetic apple juice sample, and the results are shown in Table 2.7. The determination was performed ten times with an average standard deviation of 3.8% and recovery of 99%. The accuracy of the method was further assessed by the determination of fructose in Pak Flower Honey using the APBA modified sensor and the result checked with that obtained using HPLC analysis. The results are also shown in Table 2.7. The results of both determinations demonstrated the accuracy of the determination using APBA modified QCM.

Four other honey samples were also analyzed in duplicate for their fructose contents

and the results are also shown in Table 2.7, where it can be seen that the fructose in honey samples was determined with an average recovery of 101%.

Table 2.6. Effect of some common ingredients in a synthetic apple juice sample* on the determination of fructose (5 mg/mL)

Ingredient	Concentration, %	Error, %
Ascorbic acid	0.5	5.0
Citric acid	1.5	5.0
Glucose	50	4.4
Sorbitol	10	3.8
Sucrose	50	3.4

* Composition (in 100g): glucose, 2.46g; sucrose, 1.32g; sorbitol, 0.39g; citric acid, 0.015g; ascorbic acid, 0.01g; K^{+}, 106.1mg; Na^{+}, 2.1mg; Ca^{2+}, 5.8mg; Fe^{3+}, 0.20mg; Mg^{2+}, 4.2mg; and Mn^{2+}, 0.05mg.

Table 2.7. Determination of fructose by the proposed method

Sample	Amount added	Amount found (w/w) %	Percent recovery[++]
Synthetic apple juice[•]	2.50[••]	2.48[••]	99
Honey (Pak Flower, China)	0	30.8[+]	-
Honey (Pak Flower, China)	0	31.2	-
Honey (Pak Flower, China)	10.0	41.3	101
Honey (litchi Flower, China)	0	34.8	-
Honey (litchi Flower, China)	10.0	45.0	102
Honey (Acacia, China)	0	32.7	-
Honey (Acacia, China)	10.0	42.6	99
Honey (Orange, China)	0	36.4	-
Honey (Orange, China)	10.0	46.5	101
Honey (Manuka, New Zealand)	0	38.4	-
Honey (Manuka, New Zealand)	10.0	48.5	101

• Composition as shown in Table 2.6.

•• These two data in unit of mg/mL.

+ result by HPLC analysis.

++ Average percent recovery for the honey samples is 101%.

2.3.9 Comparison with conventional saccharides sensors

Many types of saccharides sensors have thus far been constructed with enzymes. However, they have drawbacks such as high running cost of using coenzymes for the determination, and tedious cultivation and enzyme preparation procedures. Moreover, owing to the extremely high affinity between the enzymes and the target molecules, complicated elution might have to be applied to wash away the bound molecules. Owing to the poor stability of the enzymes, the lifetimes of these sensors were usually short, for instance, the response of them would dropped to half within in one week.

On the other hand, the modification procedure of sensor with synthetic ligands was much simpler, only by syringe dropping and immersion. Besides, the synthetic ligands offered low-cost alternative for saccharides sensing. The life of sensor was also prolonged since they would not undergo denaturation. In addition, ligates bound to the immobilized ligands can easily be washed away, and the sensor can recover shortly. Finally, the selectivity of the sensor could be improved to be comparable to the enzymatic sensor by modifying the structure of the ligands.

2.4 Summary

In this chapter, the concept of affinity mass sensor introduced by Shao [14] was applied to determine fructose choosing 3-aminophenylboronic acid as the affinity ligand. The performance of the sensor including its sensitivity, selectivity and stability were reported. The results obtained confirmed experimentally the viability of the affinity mass sensors. The method offers good sensitivity and reproducibility together with the added advantages of simplicity, convenience and relatively low cost.

Chapter 3

Sol-gel fabrication of affinity mass sensor

During the past decade it has become widely recognized that the sol-gel process may be used to encapsulate organometallic and biological molecules in an inorganic matrix. Notably, the comparatively mild room temperature processes of hydrolysis and condensation of alkoxides prevent decomposition of these molecules from happening. Moreover, the relative simplicity of this technology is also at least partially responsible for its rapid proliferation. Its extensive uses include biocatalysis by sol-gel entrapped enzymes, immunosensing and distinguishing environmental molecules by silicate films [49, 77].

3.1 Principle of sol-gel method

The first record of sol-gel processing was attributed to J. Ebelmen, who found that the metal alkoxide prepared from $SiCl_4$ and alcohol gelled on exposure to the atmosphere [see 78, 79]. It was later recognized by Geffcken [see 78] in the 1930s that alkoxides could be used in the preparation of oxide films. The sol-gel process is governed by the rules of chemistry. Numerous investigations showed that material properties can change drastically as a function of changing reaction parameters. The general principle of the sol-gel process is described below.

Basically, the sol-gel process means the synthesis of an inorganic network by a chemical reaction in solution at low temperature. The most obvious features of this reaction, the transition from a liquid (solution or colloidal suspension) into a solid (gel) led to the terminology "sol-gel process". Any precursor, which can form reactive "inorganic" monomers or oligomers, can be used for the sol-gel techniques. Low molecular weight alkoxysilane such as tetramethoxysilane (TMOS), tetraethoxysilane, or an equivalent organometallic alkoxide are used as precursors in most work in the sol-gel field. They provide a convenient source for "inorganic" monomers which in most cases are soluble in common solvents. These precursors react readily with water (i.e. they are hydrolyzed) as in the following reactions:

$$Si(OR)_4 + H_2O \leftrightarrow (HO)Si(OR)_3 + ROH$$

$$(HO)Si(OR)_3 + H_2O \leftrightarrow (HO)_2Si(OR)_2 + ROH$$

$$(HO)_2Si(OR)_2 + H_2O \leftrightarrow (HO)_3Si(OR) + ROH$$

$$(HO)_3Si(OR) + H_2O \leftrightarrow Si(OH)_4 + ROH$$

Depending on the amount of water and catalyst present, hydrolysis may go to completion (so that all of the OR groups are replaced by OH), or stop while they are partially hydrolyzed. Then polycondensation is followed with the liberation of small molecules such as water or alcohol:

$$\equiv Si\text{-}OH + HO\text{-}Si\equiv \leftrightarrow \equiv Si\text{-}O\text{-}Si\equiv + H_2O$$

$$\equiv Si\text{-}OR + HO\text{-}Si\equiv \leftrightarrow \equiv Si\text{-}O\text{-}Si\equiv + ROH$$

By these reactions, an inorganic backbone is built up. The gel point is defined as the point at which the entire solid mass becomes interconnected. The gel state is not a very well defined state but a gel is widely accepted as a material which, at least, is diphasic (where pores can be considered as one phase).

During the last stages of gelation, water and the organic solvent evaporate from the matrix cavities and the volume of the solid matrix shrinks gradually [48]. During the drying phase, some of the larger pores are emtied while smaller pores remain wetted by the solvent, creating large internal pressure gradients. Stress formed may lead to cracking in bulk gel, also known as monoliths. This can be solved by incorporation of surfactant. A final high temperature step treatment may be used for densification, improving the electrical conductivity, or obtaining a desirable crystallographic structure.

The sol-gel process from monomers and ending up in highly crosslinked matrices is very complex due to the high numbers of chemistry related parameters involved. For instance, the choice of precursor affects the kinetics of the reaction and the structure of oligomers. Temperature, solvent and ageing [80, 81] may also influence the solubility and the gel point. Indeed, the nature of the catalyst [82-84] and, in particular, the pH of the reaction and water content [85, 86] have a very pronounced effect on the hydrolysis and condensation reactions. Additives [87] are also added optionally to control the structure of the gel. The function of mechanical parameters cannot be underestimated too. For example, stirring and ultrasonic treatment can improve the miscibility of reagents and ensure the homogeneity of the mixture.

However, the quantitative relationship between the properties of the gel and these preparative variables is by no means straightforward and interdependencies among different properties are common. Delicate manipulation of one variable is simple, whereas tuning a set of specifications is more demanding and often requires a tedious trial-and-error process [47].

Three-dimensional inorganic matrix resulted from the sol-gel process offers several advantages including physical rigidity, high abrasion resistivity, negligible swelling in both aqueous and organic solutions, chemical inertness, photochemical and thermal stability, and excellent optical transparency.

3.2 Encapsulation of organic molecules in sol-gel matrices

Avnir, Levy and Reisfeld at Hebrew University [88] were the first to realize that moderate or even ambient temperature sol-gel process opens a way for immobilization of heat sensitive compounds by chemical doping. It is the introduction of a ligand or host molecule done by adding its solution to the polymerizing mixture. When the polymerization is completed, the dopant molecules are entangled in the inorganic polymeric network (Figure 3.1) [89]. Recent research has demonstrated that the enscapsulated ligands are accessible to external reagents through the pore network.

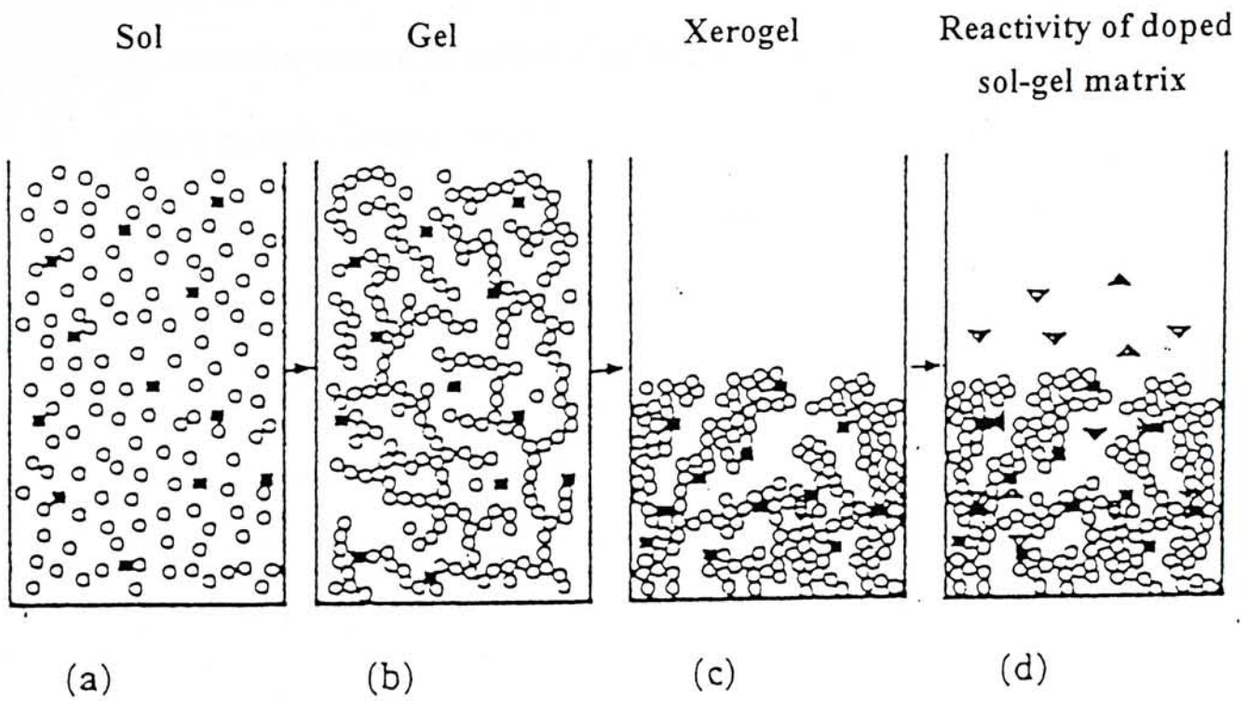

Figure 3.1. The encapsulation of dopant molecules with sol-gel matrix.

(a) A sol of inorganic oxide particles (o) was prepared by polymerization of alkoxysilane in the presence of the desired dopant molecules (▪).

(b),(c) The sol turned into a gel, which then dried, forming a porous xerogel, within which the dopant molecules were trapped.

(d) The porous network allowed external molecules (▾) to react with the trapped dopant.

Furthermore, the functionalized silicate glasses prepared are optically transparent, permitting optical monitoring of the spectroscopic properties of the encapsulated ligands. These functional glasses make it possible to retain the specificity and reactivity of the ligands in the solid state and provide morphological and structural control that is not available when the ligands are simply dissolved in aqueous media. In addition, the amorphous nature of the glassy material does not impart a geometric order to the encapsulated ligands; many of the characteristics of the liquid state are

retained despite the fact that the ligand is trapped in a solid material.

An attractive feature of sol-gel process for sensing purposes is that the organically doped inorganic matrix obtained from this process can be made in various forms, as the analytical or optical method requires. Thus, one can prepare the sensing materials as a monolithic block, as a microscopic grain, as a thin film on a flat support, as an optical fiber coating, and in chromatographic capillary tubes.

This chapter describes the preparation of sol-gel derived film with encapsulated APBA on QCM surface. Optimization of film formation conditions will also be investigated. Fructose sensing will be demonstrated by using this affinity mass sensor and the performance of the sensor will also be evaluated. At the end of this chapter, sensors fabricated with two different methods, namely the crosslinking method (discussed in Chapter 2) and sol-gel method, will be compared.

3.3 Experimental

3.3.1 Preparation of alkoxide solutions

Tetraethyl orthosilicate (TEOS), Triton-x-100 and 3-aminophenylboronic acid were purchased from Acros. Hydrochloric acid, ammonia, ethanol, D-glucose, sucrose and maltose were obtained from BDH. Ammonium acetate, for preparation of the buffer, and D-fructose were from Merck. All chemicals were used as received, and all water used was purified using a Millipore purification system.

In all sol-gel stock solutions, tetraethyl orthosilicate (TEOS) was used as the sol-gel precursor. Water was added for the hydrolysis reaction. Ethanol acted as a common solvent to ensure the mixture to be homogeneous and one drop of Triton-x-100 was applied as surface active agent. 3-aminophenylboronic acid (APBA) was added to each mixture except for the control.

For optimization of the composition of the sol-gel mixture, different mixtures were prepared, each of which contained 1 mL of TEOS, 0.05 mL of the catalyst, 1 drop of Triton-x-100 and varying amounts of water as shown in Table 3.1. To obtain clear solution mixtures without any precipitation, ethanol was added to each sol-gel mixture such that the total volume of the mixture was controlled to be 5 mL. Appropriate amount of APBA was first dissolved in water such that the concentration of APBA in each resulting mixture was as shown in Table 3.1. In order to assess appropriate catalyst for the formation of sol-gel derived film, mixture *1* and *2* were prepared in which 0.05 mL of dilute hydrochloric acid and aqueous ammonia was added as catalyst respectively under constant stirring.

Another series of mixtures with different water to alkoxysilane ratios were prepared. The water contents were adjusted so that the mole ratios of water to alkoxysilane increased from two for mixture *3* to forty for mixture *8*. The ratio of two corresponded to the amount of water required for complete polycondensation. Sol-gel mixtures *9* to *14* with different ligand (APBA) loading amounts were also prepared.

Table 3.1. Composition of starting sol used in this study

Sol mixture	Catalyst (0.05 mL)	TEOS (mL)	H_2O (mL)	H_2O (including that in catayst):TEOS mole ratio, *R*	Conc. of APBA in resulting mixture(mg/mL)
1	0.1 M HCl	1	0.11	2	10
2	0.05 M NH_3 (aq.)				
3	0.1 M HCl	1	0.11	2	10
4			0.27	4	
5			0.43	6	
6			0.75	10	
7			1.55	20	
8			3.15	40	
9	0.1M HCl	1	0.11	2	0
10					5
11					10
12					15
13					20
14					25

Ethanol was added as the common solvent and the total volume of each sol mixture was controlled to 5 mL and 1 drop of Triton-x-100 was added to each sol mixture.

3.3.2 Film deposition on QCM

For homogeneous wetting of the surface of the QCM, it should be cleansed thoroughly with piranha solution with great care before coating. *Caution: piranha solution reacts violently with most organic materials and must be handled with extreme care.* The QCM was dipped in the sol with the optimized composition and then pulled out and placed horizontally. The liquid film partly flowed down the QCM

and partly adhered to it. It was stored in a desiccator to dry. The sensor was then ready to be mounted in the flow cell for analysis following the same procedures as described in **2.2.5** in Chapter 2.

3.3.3 Film characterization and surface analysis

Characterization of sol-gel derived film with APBA encapsulated was performed with Nicolet Impact 420 FT-IR spectrometer. The film was peeled off from a coated surface, and was then ground into powder and compacted with dry potassium bromide under pressure in *vacuo* to form a transparent disk.

The successful encapsulated of APBA in the film was also evidenced by X-ray photoelectron spectroscopy (XPS). The measurements of XPS were performed using a PHI Quantum 2000 ESCA microprobe apparatus equipped with a monochromatized Al Kα source (1486.5 eV) under high vacuum of 2.0×10^{-9} Torr. The instrument was calibrated to 84.00eV for Au 4f. Sputtering was also performed with Ar+ ion at 4 keV.

Study of surface morphology of the film on QCM was done by scanning electron microcopy (SEM). It was performed on a Cambridge Stereroscan 360 operated at 20 kV equipped with an Oxford microprobe attachment. The QCM was supported on a graphite plate and fixed with a conducting adhesive tape.

3.4 Results and Discussion

3.4.1 Optimization of conditions for the sol-gel process

3.4.1.1 Choice of catalyst

It is known that acids promote the rate of hydrolysis more than the polycondensation reaction in the sol-gel process. Thus, the gel time was relatively long for acid catalyzed process. The gel evolved tended to be weakly crosslinked as shown in Figure 3.2a.

In contrast, a base promotes the polycondensation reaction more than the hydrolysis reaction. The polycondensation reaction created additional bridging bonds and increased the viscosity. This led to shorter gelation time for base catalyzed system. Thus, mixture *2* catalyzed by NH_3(aq) was clear just after preparation but became cloudy shortly. This made uniform coating on electrode surface of the QCM impossible. The resultant gel was less clear than the gel from mixture *1*. Hence, a basic environment tends to produce more of a dense-cluster growth leading to dense particulate-like structures. These particles would later bridge to form a very inhomogeneous system as shown in Figure 3.2b.

Therefore, acid catalyzed sol-gel process with the use of dilute HCl would be applied instead of base catalyzed process in this study.

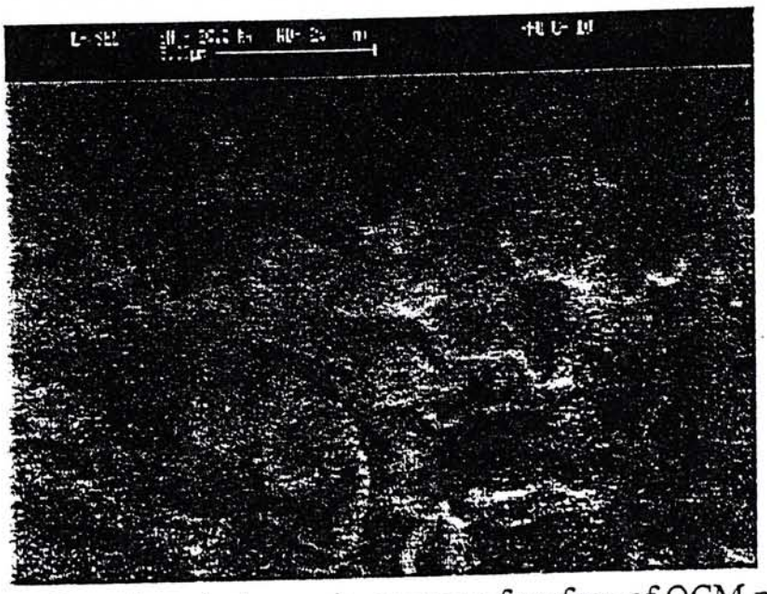

Figure 3.2a. Scanning electron microscopy of surface of QCM modified with sol mixture *1* (hydrochloric acid as catalyst).

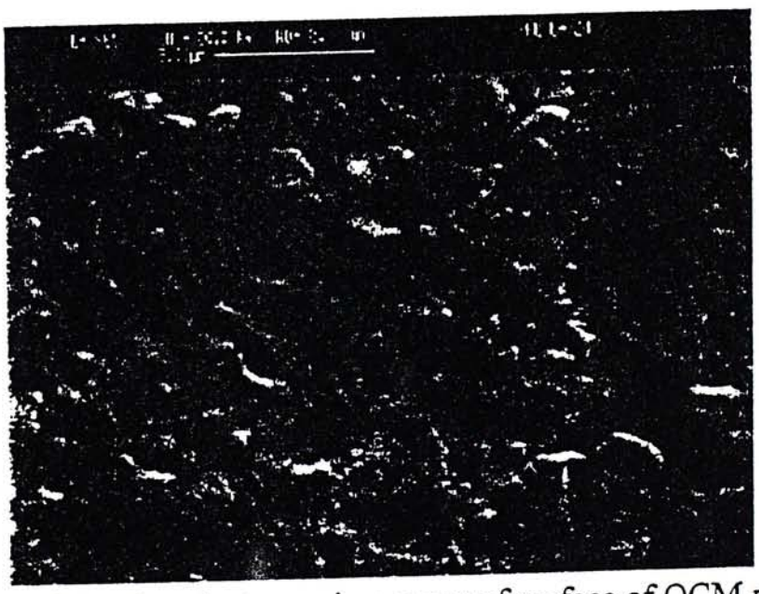

Figure 3.2b. Scanning electron microscopy of surface of QCM modified with sol mixture *2* (aqueous ammonia as catalyst).

3.4.1.2 *H_2O : TEOS ratio, R*

Because the mole ratios of H_2O/TEOS (denoted *R*) were different in mixtures *3* to *8*, different gel networks were created. Figure 3.3 revealed the effect on the sensor response by different *R* values. For the system with higher R value, the hydrolysis reaction would occur more rapidly and more completely. Keefer [see 85] found that a surface fractal structure was formed. Whereas for incomplete hydrolysis, a mass fractal resulted, where mass fractals were those objects which had holes on every length scale. Thus, the hydrolyzed species for high R values would be rapidly incorporated into the forming clusters, leading to a more polycondensed and less porous network. As a result, the ligands immobilized in such gel matrix would be less accessible due to low porosity, leading to lower response of the sensor. In other words, low *R* value mixture would be preferred in the fabrication of the sensor, and an *R* value of 2 was chosen.

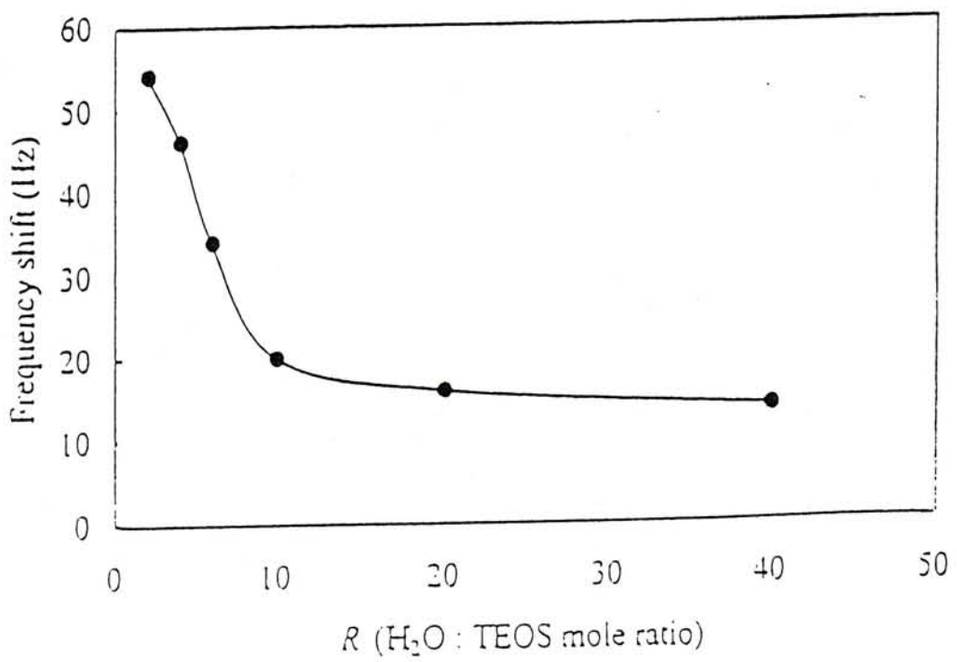

Figure 3.3. Peak response of the sensor to fructose (3 mg/mL) as a function of H_2O : TEOS mole ratio.

3.4.1.3 *Ligand loading*

The amount of APBA encapsulated into the sol-gel film on the QCM influences the amount of fructose that can be bound to the surface and hence the resulting response of the sensor. As shown in Figure 3.4, the response increased sharply upon raising the APBA loading to 10 mg/mL (in the sol-gel solution) and then it started to level off. Such a profile reflected the saturation of the surface-exposed binding sites of APBA. Hence, an APBA loading of 10 mg/mL was used to construct the sensor for the following experiments.

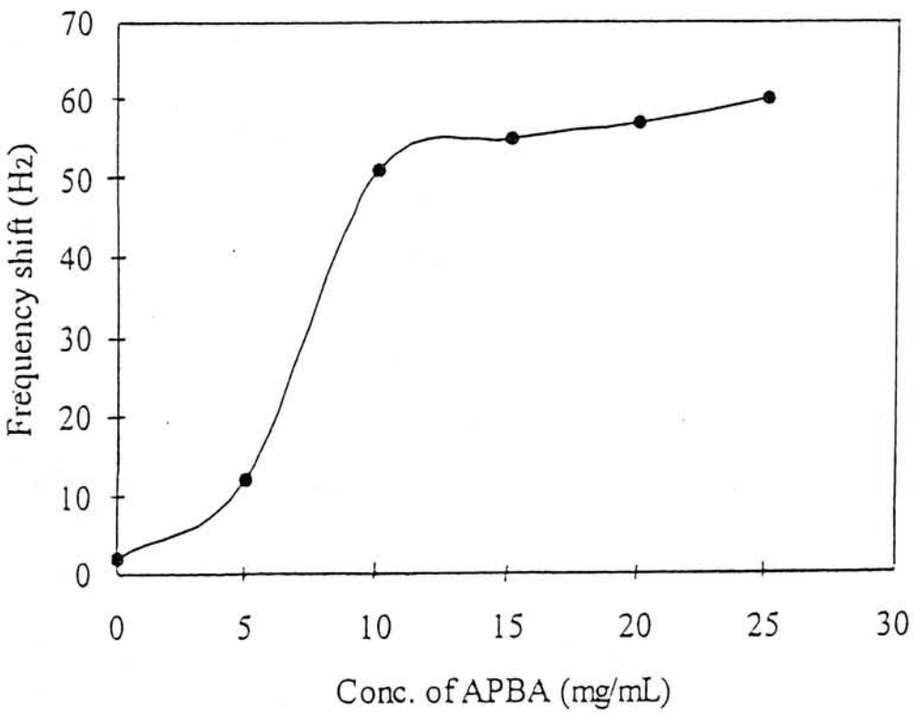

Figure 3.4. Peak response of the sensor to 3 mg/mL fructose as a function of APBA concentration.

3.4.1.4 *Surface active agent*

The addition of Triton-x-100 as the surface active agent (SAA) resulted in greatly improved homogeneity of the sol mixture. Another significant function of SAA was

to decrease the tensions built within the film during polymerization, so that cracking of the film could be avoided.

In summary, the optimized H_2O/TEOS ratio was 2, the total volume of sol was kept to 5 mL with ethanol as solvent. The pH of the sol was adjusted to 2 with 0.1 M HCl and 1 drop of Triton-x-100 was added. The optimum loading of APBA was 10 mg/mL.

3.4.1.5 *Temperature*

Sols with the above optimized composition were heated at different temperatures. Figure 3.5 describes the effect of temperature on the response of the sensor, where little variation in response was observed. This was due to the fact that at low pH, the particle size was less dependent on solubility, which was partly governed by temperature. Hence, the temperature has little impact on the structure of the film derived from acid catalyzed sol-gel process. For convenience, the preparation of sol for sensor fabrication was performed at room temperature.

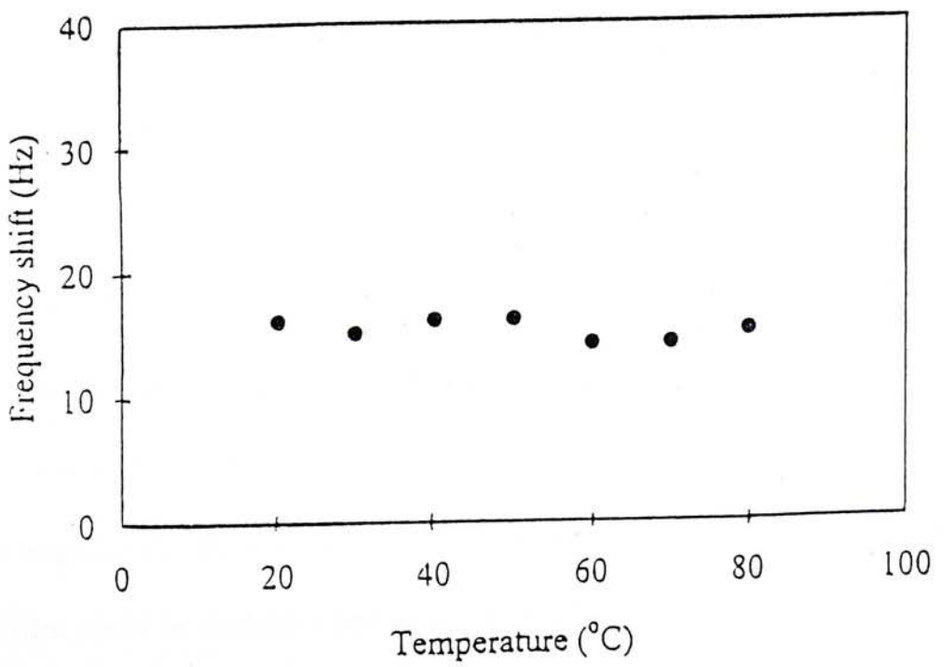

Figure 3.5. Peak response of the sensor to 1 mg/mL fructose as a function of temperature at which the sol heated.

3.4.1.6 *Ageing and drying*

The structural evolution of sol-gel derived thin films differed in many aspects from that of bulk sol-gels. In the case of films, the hydrolysis/condensation stage might overlap the deposition stage, resulting in gelation and drying occurring simultaneously. Due to the rapid drying of the thin film, the gel ageing processes, which enhance the porosity of monolithic gels, does not occur to the same extent. Therefore, a sol ageing or pre-polymerization process was carried out by allowing the sol to stand at room temperature. For sensor coated with sol that was aged for a few hours, a large fluctuation (over 10 Hz) was observed for the baseline when the sensor was mounted in flow cell with buffer solution running through the cell. Under the same operation, stable baseline (less than 1 Hz fluctuation) could easily be obtained with a sensor coated with 5-day-aged sol. This indicates that the film produced from aged sol exhibits higher stability. Besides, the increase of pre-polymerization time enhanced encapsulation of the ligands in the matrix. This lowered the leaching of ligands. For sensor aged for a few hours, the response to the same sample solution dropped to nearly half after the first operation in the aqueous phase, whereas the responses for the sensor aged for 5 days were steady in continuous operation for over 1 hour.

3.4.2 Characterization of APBA encapsulated film

Figure 3.6a & 3.6b depicted the spectra of pure APBA and sol-gel film doped with APBA respectively. By comparing the two spectra, the FT-IR spectrum of the APBA doped film could be characterized by the peaks listed in Table 3.2 [90-92].

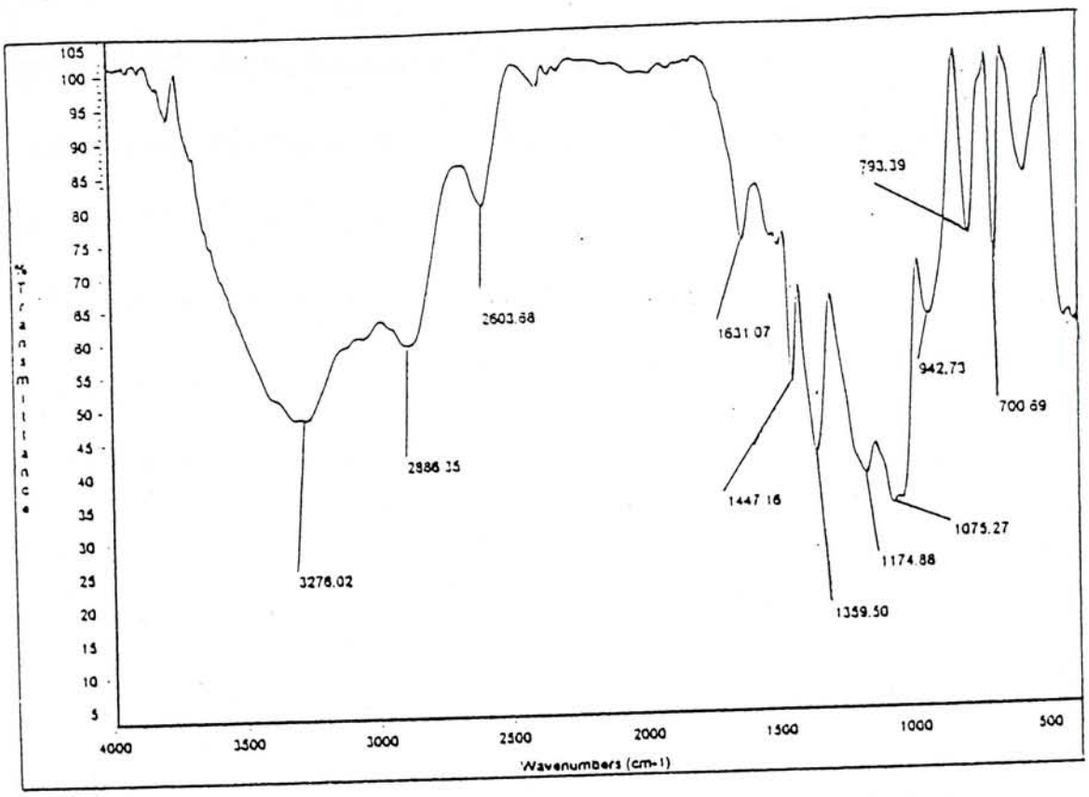

Figure 3.6a. FT-IR spectrum for APBA doped sol-gel derived film.

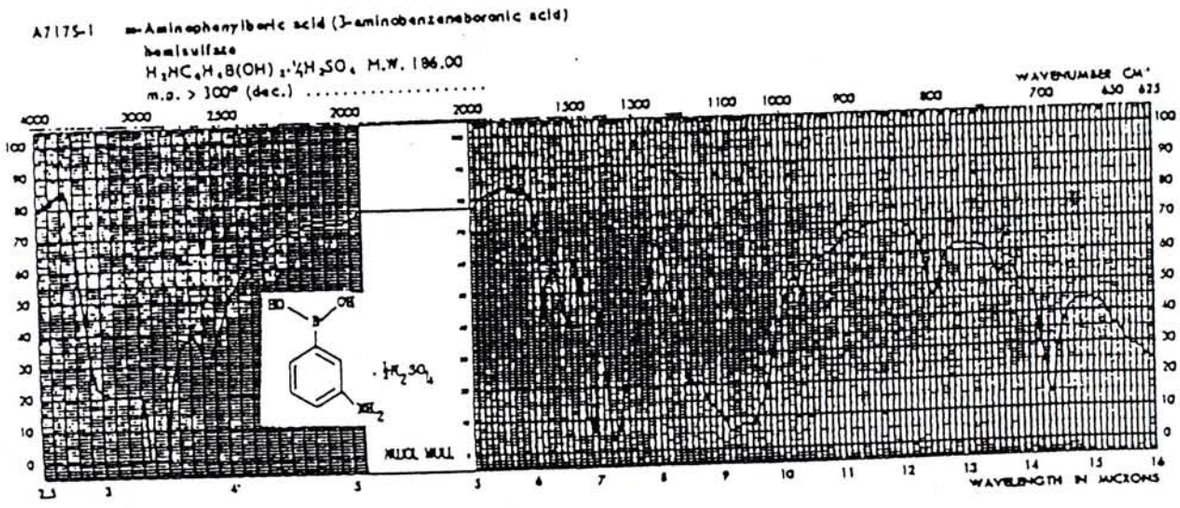

Figure 3.6b. IR spectrum for pure APBA (from refernece [91]).

The surface of the QCM coated with APBA doped sol-gel film was also examined with XPS. The results are shown in Table 3.3, which revealed the presence of boron and nitrogen atoms, indicating that the film had incorporated APBA. The observed oxygen peak was caused by the oxygen from the siloxane bonds in the network and in hydroxyl groups of APBA molecules. The peak position of B 1s was found to be 193.11 eV. According to the handbook of XPS [93], boron bound to electronegative species would have binding energy between 192.0 to 193.3. From the result, it was reasonable to deduce that boron in the sol-gel film was bound to oxygen. Hence, the B-O bonding was believed to exist to facilitate the cyclic ester formation with fructose in sample solution.

Table 3.2. Characteristic peaks of FT-IR spectrum for APBA doped sol-gel derived film.

Origin of peaks	**Wavenumbers (cm^{-1})**
APBA	2886, 2604, 1631, 1447, 1360, 1174, 793, 701
Si-O-Si	1075

Table 3.3. Elemental compositions found by XPS

Element	**Atomic %**
O (1s)	50.0
Si (2p)	29.0
C (1s)	14.3
B (1s)	2.6
N (1s)	2.6
Pt (4f)	1.4

Further evidence of successful encapsulation of APBA in the film could be given by the response curve shown in Figure 3.7. The sensor modified with sol-gel film in which no APBA was encapsulated (from mixture *9*) acted as a control, and it gave only 2 Hz response for 5 mg/mL fructose solution. While the response of the sensor coated with APBA doped sol-gel film was found to be 82 Hz. This large frequency drop was attributed to the specific binding between fructose in the sample solution and the APBA entrapped in the sol-gel film on the QCM surface.

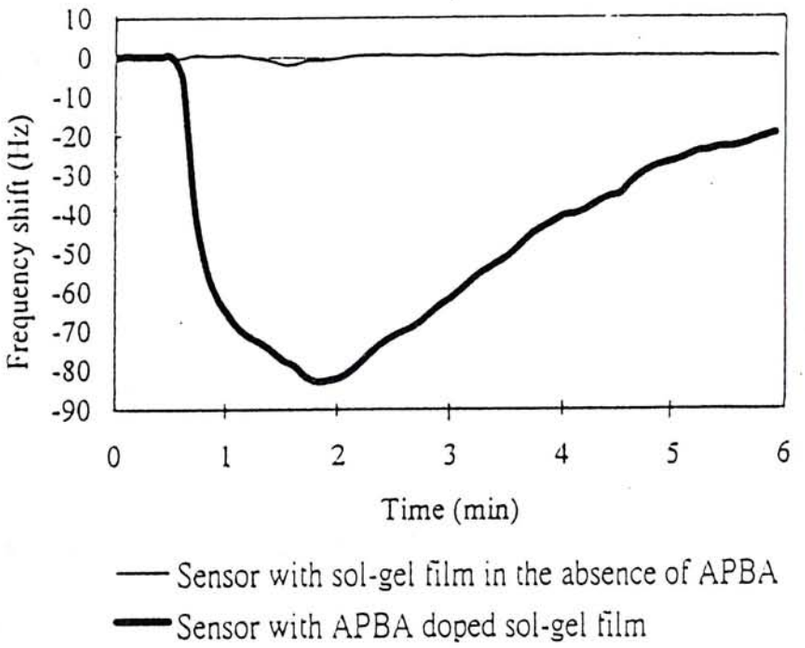

Figure 3.7. Response of QCM modified with APBA doped sol-gel film to fructose (5 mg/mL).

3.4.3 Performance of the sol-gel derived sensor

3.4.3.1 *Calibration*

A sensor prepared with APBA doped sol-gel film was tested for its response to different concentrations of fructose. These data are shown graphically in Figure 3.8.

A linear relation between the response and fructose concentration was found in the range of 0.1 mg/mL to 10 mg/mL with a correlation coefficient of 0.999. The lower limit of reliable detection was determined to be 2 Hz for a signal to noise ratio of 3, and the corresponding concentration was 7×10^{-2} mg/mL.

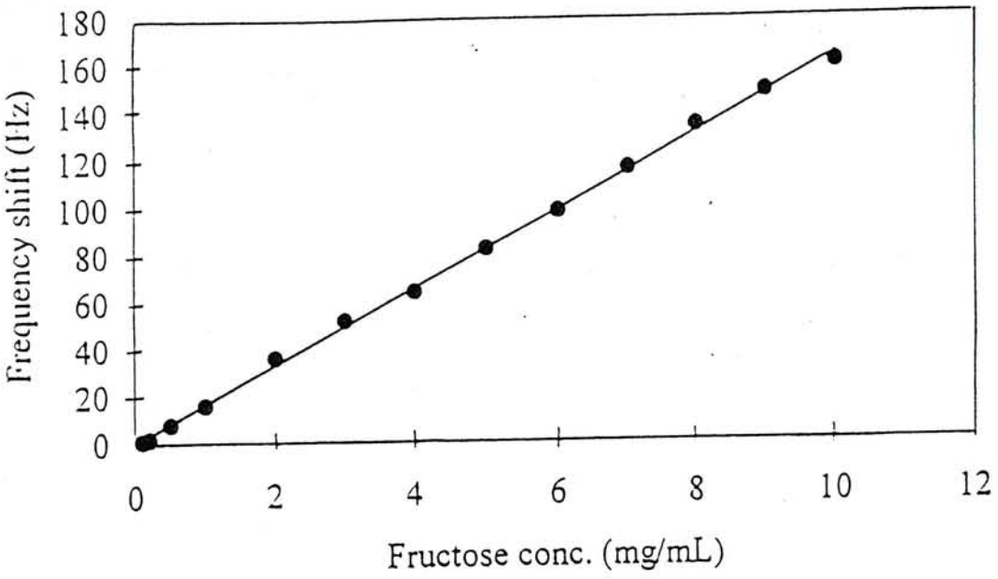

Figure 3.8. Response of sensor modified with APBA doped sol-gel film to fructose solutions with different concentrations.

3.4.3.2 *Stability*

Since the interest of this study was in developing a sensor operated in the aqueous phase, the stability of the sensor had been investigated by measuring its response to 5 mg/mL fructose solution in water in a continuous-operation mode. From Figure 3.9, no apparent change in response was observed over a period of 90 minutes. The relative standard deviation for these 10 replicate injections was 1.0% at 5 mg/mL fructose level. After the above continuous measurements, the sensor was dismounted from the flow cell, rinsed with water and then dried. The weight loss of the film on the sensor was found to be less than 5%.

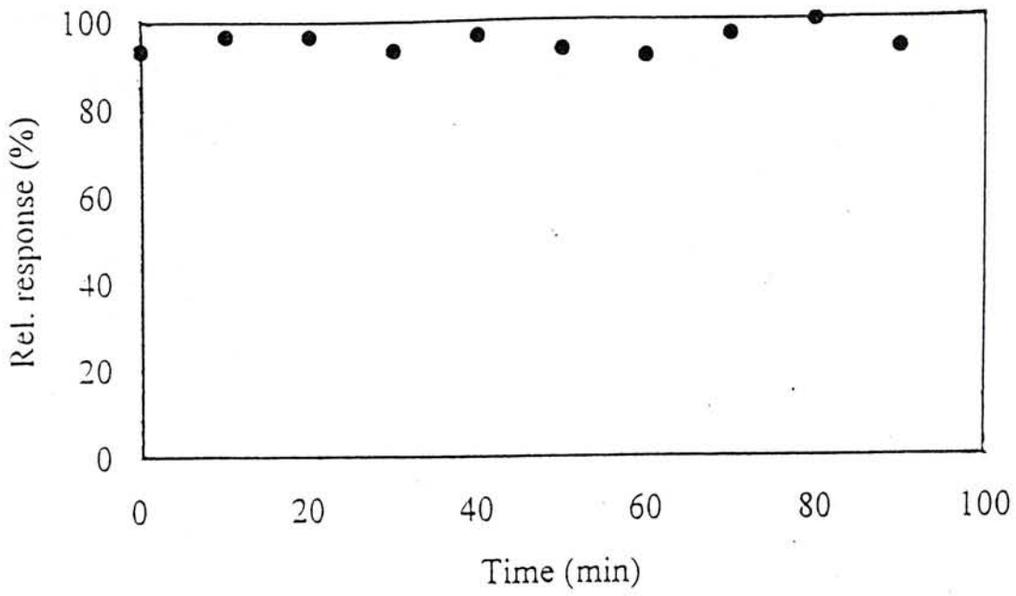

Figure 3.9. Relative response of the sensor to 5 mg/mL fructose in a continuous-operation mode.

The response of the sensor to fructose was also observed over a period of 2 months. In these experiments, the flow cell which housed the sensor was disconnected from the pumping system after each working period. From Figure 3.10, it can be seen that after the first week, the response of the sensor was found to remain 90% of its original value.

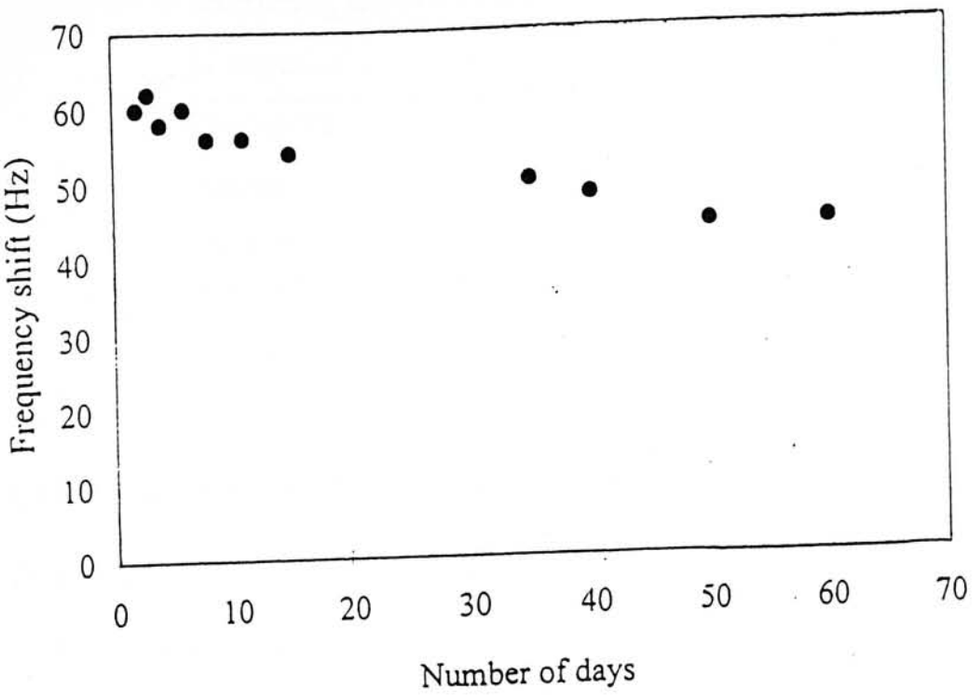

Figure 3.10. Stability of the sensor under storage (response to 5 mg/mL fructose).

3.2.3.3 *Selectivity*

Another important aspect that should be studied was the selectivity of the encapsulated ligand. Since honey was chosen to demonstrate the practical usage of the sensor, the sensor was thus exposed to fructose solutions in the presence of three sugars found in honey which may interfere with the determination.. From Table 3.4, the relatively low interference caused by these species suggested that the selectivity of the APBA encapsulated in the silicate matrix was retained.

Table 3.4. Effect of some other saccharides also found in honey on the determination of fructose (5.00 mg/mL).

Interfering species added (1 mg/mL)	Conc. detnd.	+ve error (%)
D-glucose	5.03	0.7
surcose	5.12	2.4
maltose	5.12	2.4

3.4.4 Applicability of the sol-gel derived sensor

To test the sensor in a real sensing application, five honey samples were analyzed. Table3.5 summarized the results obtained by standard addition method, and measurements were done in duplicate.

Table 3.5. Fructose contents in honey samples

Sample	Conc. detnd. by sol-gel film modified sensor (w/w%)
Pak Flower (China)	31.3 ± 0.6
Litchi Flower (China)	35.8 ± 0.6
Acacia (China)	33.0 ± 0
Orange (China)	37.0 ± 0.6
Manuka (New Zealand)	39.2 ± 0.6

3.4.5 Comparison between sensors fabricated via the crosslinking method and the sol-gel method

3.4.5.1 *Surface uniformity*

In an attempt to apply a liquid coating on the surface of QCM, the two common methods are syringe dropping and dipping. In the crosslinking immobilization method described in Chapter 2, APBA was immobilized by applying a drop of PEI solution with a microsyringe to the center of one side of the QCM, and the liquid spread over the QCM, mainly in the central part of the electrode, but not in the same way throughout the whole area. The film was non-uniform as can be seen from Figure 3.11. In contrast, as shown in Figure 3.12, the film produced by dip coating with the sol mixture exhibited higher uniformity over the electrode area of the QCM.

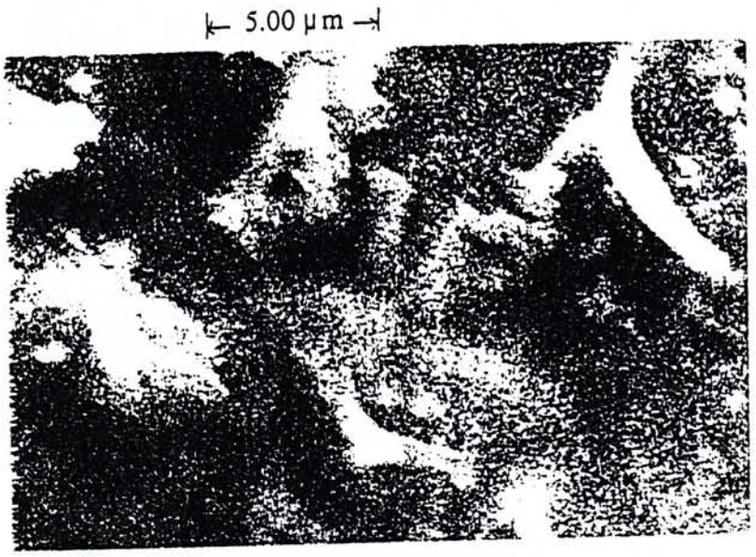

Figure 3.11(a)

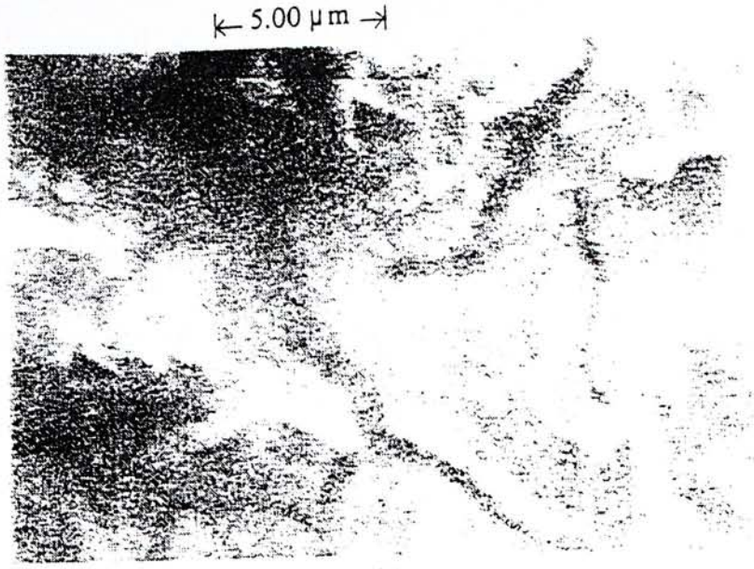

(b)

Figure 3.11 Scanning electron microscopic images (Mag = x 5.03 K) of two different regions of the crosslinking modified QCM surface,
(a) at center of electrode & (b) at the rim of the electrode.

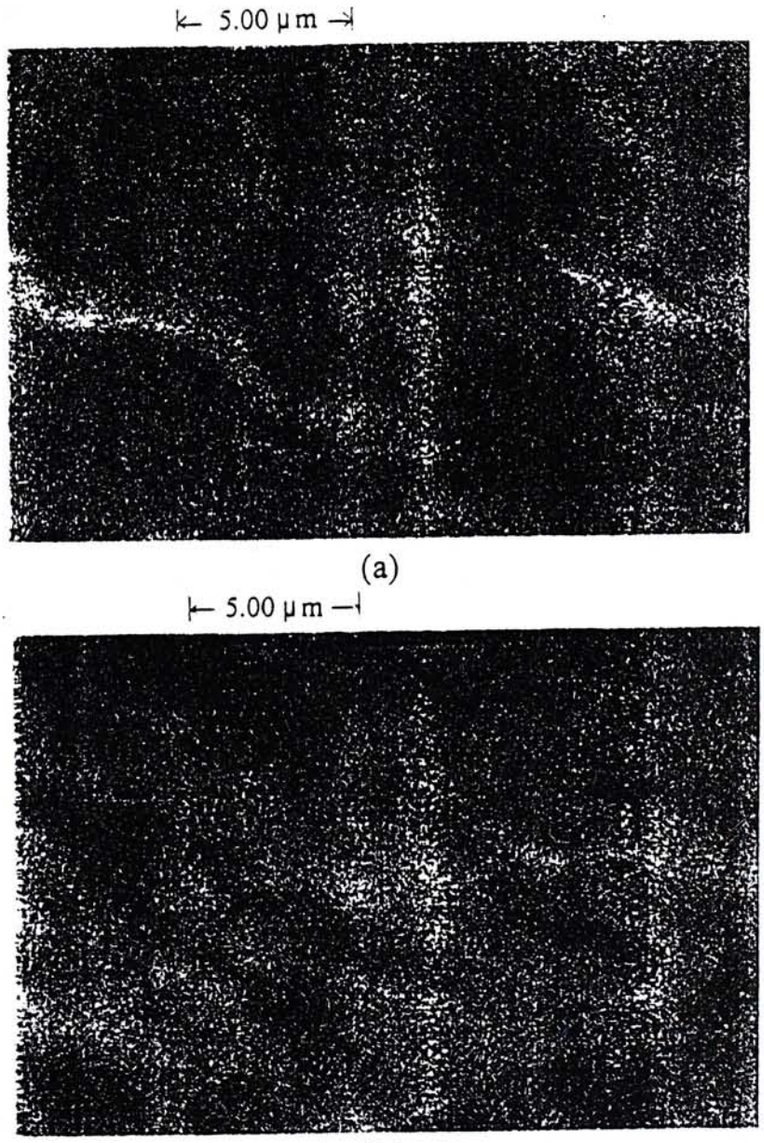

(a)

(b)

Figure 3.12 Scanning electron microscopic images (Mag = x 5.05 K) of two different regions of the sol-gel modified QCM surface,
(a) at center of electrode & (b) at the rim of the electrode.

3.4.5.2 *Reproducibility in mass deposition*

For both the crosslinking and sol-gel methods, the coating procedures were carried out using batches of ten QCMs. The frequency decreases due to coating for these QCMs were recorded and presented in Table 3.6. In practice, the QCMs show greater mass sensitivity at the center of the electrodes, and the sensitivity decreases monotonically with the radius in a Gaussian manner [94]. With the syringe method, a slight difference in positions of the drop cast from one QCM to the other caused a large variation in the frequency changes. In the dip coating method, the control of volume and position of droplet casting on each QCM could be avoided. Hence, the relative standard deviation for the frequency changes due to coating method obtained with dip coating method was much lower than that obtained with syringe method.

Table 3.6. Comparison of the reproducibility of the two immobilization methods

	Crosslinking by glutaraldehyde	Sol-gel film
Average freq. shift for a batch of 10 QCMs (kHz)	76.9	30.8
SD (kHz)	9.6	0.4
RSD (%)	12.5	1.3

3.4.5.3 *Stability*

As mentioned in the last chapter, the sensor modified with the crosslinking method could overcome the general short life of conventional enzymatic sensors. It retained 80% of its sensitivity after one week. The stability of the sensor prepared using the

sol-gel method was further enhanced. The response of the sensor dropped less than 10% at the end of the first week. This suggests that leaching of the ligand was an inherent problem resulting in the loss of sensitivity. The long-term stability of doped silicate sensor was comparable to sensor fabricated by crosslinking method because the ligands were isolated from the surroundings by a matrix with small pores.

3.4.5.4 *Sensitivity towards fructose standard*

The comparison of sensitivity between sensors fabricated by the crosslinking method and the sol-gel method can be made from the calibration curves for sensors modified by both methods. The larger the slope, the higher the sensitivity of the sensor. From Figure 2.12 (calibration curve of the crosslinking fabraicated sensor) and Figure 3.8 (calibration curve of the sol-gel fabricated sensor), the value of slopes were found to be 57.5 Hz mL/mg and 16.3 Hz mL/mg respectively. Hence, a more sensitive sensor can be fabricated through the crosslinking method.

3.4.5.5 *Comparison of precision and accuracy*

In order to compare the precision of the fructose detection by two kinds of modified QCMs, an *F* test was performed:

$$F_{observed} = s_{crosslinking}^2 / s_{sol\text{-}gel}^2 \qquad \text{equ.3.1}$$

For the determination of fructose content in standard solution by the method of standard addition, by using a data set with 9 degrees of freedom, the relative standard deviation for crosslinking modified sensor, $s_{crosslinking}$, and the relative standard deviation for sol-gel modified sensor, $s_{sol\text{-}gel}$, were determined to be 1.5% and 1.0%

respectively. As a result $F_{observed}$ was calculated to be 2.25. This value is smaller than the critical F value of 3.18, hence no significant difference between the precision of two types of sensors has been demonstrated.

For the fructose sensing with two different kinds of modified QCMs, the measurements were made in exactly the same way. The accuracy of the method using these two kinds of QCMs was compared by the differences obtained in the determination of fructose in five honey samples and as shown below.

Table 3.7. Comparison of results of determination of fructose in five honey samples obtained with two different kinds of modified QCMs

	Deviation* from the value obtained using sensor fabricated through crosslinking in Chapter 2 (w/w%)
Pak flower	0.1 (0.3)
Litchi flower	1.0 (2.9)
Acacia	0.3 (0.9)
Orange	0.6 (1.6)
Manuka	0.8 (2.1)

* using data in Table 2.7 and the relative deviation is shown in parenthesis.

The difference in results for each type of sample determined using the two kinds of sensors were within 1w/w% and relative deviation of 3%, indicating that the accuracy using both sensors are comparable.

3.5 Summary

Sol-gel technique was used to immobilize the affinity ligand, 3-aminophenylboronic acid (APBA), on the surface of QCM by encapsulation in stable porous inorganic matrix under mild conditions. The ligate (fructose in this study) was allowed to access APBA encapsulated in the sol-gel derived film such that the affinity reaction could easily be monitored by mass change of this affinity mass sensor. The present study showed that the properties of the sol-gel modified sensor depended on the optimized sol composition and the conditions for deposition. Besides, the encapsulated ligand was proven to be able to retain its binding activity and selectivity within the inert matrix. Finally, the results for the determination of fructose in real samples using sensors prepared by the sol-gel method and that fabricated with crosslinking method described in Chapter 2 were compared and no significant difference in accuracy was detected. A summary of the comparison of the performance of the sol-gel modified sensor and the sensor fabricated by crosslinking immobilization is shown in Table 3.8 on next page, where it can also be seen that the sensor prepared by the sol-gel method has a more uniform mass deposition in the fabrication process and a comparable precision, but poorer sensitivity in detecting fructose where compared with the sensor fabricated through crosslinkage.

Table 3.8. Summary of comparison between sensors fabricated by crosslinking method and sol-gel method

	Sensor fabricated by crosslinking method	Sensor fabricated by sol-gel method
Sensitivity (Hz mL/mg)	57.5	16.3
RSD for mass deposition in the fabrication process (%)	12.5	1.3
RSD for 10 replicate injections of 5 mg/mL fructose (%)	1.5	1.0
Honey sample results: (w/w%)		
Pak flower, China	31.2	31.3
Litchi flower, China	34.8	35.8
Acacia, China	32.7	33.0
Orange, China	36.4	37.0
Manuka, New Zealand	38.4	39.2

Conclusion

Quartz crystal microbalance has been described as a double-edged sword because anything that has mass can generate a response to the device, so the range of potential applications is very wide. The downside of this universal response is the danger of interferences. Affinity mass sensor is a QCM on which affinity ligands with selectivity are immobilized, which sheds light on solving this problem. 3-aminophenylboronic acid and fructose were chosen as the affinity ligand and the corresponding ligate to verify the concept of affinity mass sensor developed by Shao [14] in this study.

The immobilization of affinity ligand APBA through glutaraldehyde crosslinking was described. For analysis in the liquid phase, the sensor was mounted in a flow through cell. The effects of operating parameters on the performance of the sensor were studied systematically and the results agreed with numerical simulation results established by Shao [14]. In addition, the sensor was made to be sensitive and reusable by choosing an affinity reaction with suitable association rate constant and dissociation rate constant respectively. Good precision was observed from results of repeated measurements of fructose standard solution. Moreover, satisfactory results have been obtained for determination of fructose in honey samples.

The sol-gel technology has been proved to be an efficient tool for obtaining inorganic matrices useful in diverse analytical applications. It was applied to derive films on the QCMs. Affinity ligand APBA was encapsulated in such film to facilitate fructose

sensing. Via this method, more reproducible immobilization could be achieved. The porous nature of the film allowed access of fructose to APBA forming ester complex. The influences of several parameters on sensor response were investigated. Besides, the operation range was examined. The resulting sensor offered stability in continuous operation and relatively long life.

The sol-gel derived sensor promised to compete well with the sensor fabricated by crosslinking immobilization method. Although, in this work, only APBA-based sensor was exemplified, the versatility of the sol-gel process promises that other chemical sensors will soon emerge, benefiting from the favorable properties of the silicate matrices and the molecular design of artificial ligands.

References

1. Spichiger-Keller, U. E. *Chemical Sensors and Biosensors for Medical and Biological Applications*; Wiley: Chichester, 1998.

2. Valcárcel, M.; Luque de Castro, M. D. *Flow-Through (Bio)chemical Sensors*; Elsevier: Netherlands, 1994; pp 13-45.

3. Kriz, D.; Ramström, O.; Mosbach, K. *Anal. Chem. News & Features* **1997**, 345A-349A.

4. Göpel, W. *Sens. Actuators, B* **1994**, *18-19*, 1-21.

5. Janata, J.; Josowicz, M. *Anal. Chem.* **1998**, *70*, 179R-208R.

6. Buerk, D. G. *Biosensors : Theory and Applications*; Technomic: Lanchaster, 1993.

7. Henry, C. *Anal. Chem. News & Features* **1998**, 594A-598A.

8. Wang, J. *Anal. Chem.* **1995**, *67*(12), 487R-492R.

9. Rogers, K. R. *Biosens. Bioelectron.* **1995**, *10*, 533-541.

10. Dietrich, A. M.; Jensen, J. N.; da Costa, W. F. *Water Environ. Res.* **1996**, *68*(4), 391-406.

11. Minunni, M.; Mascini, M.; Guilbault, G. G.; Hock, B. *Anal. Lett.* **1995**, *28*(5), 749-764.

12. Schneider, T. W.; Frye, G. C.; Martin, S. J.; Spates, J. J. *Anal. Chim. Acta* **1995**, *309*, 53-62.

13. Barzana, E. *Adv. Biochem. Eng./Biotechnol.* **1996**, *53* (Down-stream Processing Biosurfactants/ Carotenoids), 1-15.

14. Shao, B., Doctoral Thesis, The Chinese University of Hong Kong, 1997.

15. Buttry, D. A.; Ward, M. D. *Chem. Rev.* **1992**, *92*, 1355-1379.

16. Lu, C.; Czanderna, A. W. Eds. *Applications of Piezoelectric Quartz Crystal Microbalances*; Elsevier: Amsterdam, 1984.

17. Grate, J. W.; Martin, S. J.; White, R. M. *Anal. Chem.* **1993**, *65*(21), 940A-948A.

18. Schumacher, R. *Angew. Chem. Int. Ed. Engl.* **1990**, *29*, 329-343.

19. Thompson, M.; Kipling, A. L.; Duncan-Hewitt, W. C.; Rajakovic, L. V.; Cacic-Vlasak, B. A. *Analyst* **1991**, *116*, 881-890.

20. Oberg, P.; Linensjo, J. *Review of the Scientific Instruments* **1959**, *30*, 1053.

21. Aoki, K.; Brousseau, L. C.; Mallouk, T. E. *Sens. Actuators, B* **1993**, *13-14*, 703-704.

22. Nanto, H.; Tsubakino, S.; Habara, M.; Kondo, K.; Morita, T.; Douguchi, Y.; Nakazumi, H.; Waite, R. I. *Sens. Actuators, B* **1996**, *34*, 312-316.

23. Nomura, T.; Okuhara, M. *Anal. Chim. Acta* **1982**, *142*, 281-284.

24. Kanazawa, K. K.; Gordon, J. G. *Anal. Chim. Acta* **1985**, *175*, 99-105.

25. Konash, P. L.; Bastiaans, G. J. *Anal. Chem.* **1980**, *52*, 1929-1931.

26. Mo, Y.; Hwang, E.; Scherson, D. A. *J. Electrochem. Soc.* **1996**, *143*(1), 37-43.

27. McCaffrey, R. R.; Bruckenstein, S.; Prasad, P. N. *Langmuir*, **1986**, *2*, 228-229.

28. Schneider, T. W.; Buttry, D. A. *J. Am. Chem. Soc.* **1993**, *115*, 12391-12397.

29. Calvo, E. J.; Danilowicz, C.; Etchenique, R. *J. Chem. Soc. Faraday Trans.* **1995**, *91*(22), 4083-4091.

30. Ivanchenko, M. I.; Kobayashi, H.; Kulik, E. A.; Dobrova, N. B. *Anal. Chim. Acta* **1995**, *314*, 23-31.

31. Lin, Z.; Ward, M. D. *Anal. Chem.* **1996**, *68*(8), 1285-1291.

32. Suleiman, A. A.; Guilbault, G. G. *Anal. Lett.* **1991**, *24*(8), 1283-1292.

33. Yun, K.; Kobatake, E.; Haruyama, T.; Laukkanen, M. L.; Keinänen, K.; Aizawa, M. *Anal. Chem.* **1998**, *70*, 260-264.

34. McCallum, J. J. *Analyst* **1989**, *114*, 1173-1189.

35. Muratsugu, M.; Ohta, F.; Miya, Y.; Hosokawa, T.; Kurosawa, S.; Kamo, N.; Ikeda, H. *Anal. Chem.* **1993**, *65*, 2933-2937.

36. Bao, L.; Deng, L.; Nie, L.; Yao, S.; Wei, W. *Anal. Chim. Acta* **1996**, *319*, 97-101.

37. Wang, J.; Jiang, M.; Nilsen, T. W.; Getts, R. C. *J. Am. Chem. Soc.* **1998**, *120*, 8281-8282.

38. Kooyman, R. P. H.; van den Heuvel, D. J.; Drijfhout, J. W.; Welling, G. W. *Thin Solid Films*, **1994**, *244*, 913-916.

39. Rickert, J.; Weiss, T.; Göpel, W. *Sens. Actuators, B* **1996**, *31*, 45-50.

40. Paolesse, R.; Natale, C. D.; Macagnano, A.; Davide, F.; Boschi, T.; D'Amico, A. *Sens. Actuators, B* **1998**, *47*, 70-76.

41. Ulman, A. *An Introduction to Ultrathin Organic Films: From Langmuir-Blodgett to Self-Assembly*; Academic Press: Boston, 1991.

42. Petty, M. C. *Langmuir-Blodgett Films: An Introduction*; Cambridge University Press: Cambridge, 1996.

43. Grandke, T.; Ko W. H. Eds. *Sensors: A Comprehensive Survey, Volume 1 Fundamentals and General Aspects*; VCH: New York, 1989.

44. Sugimoto, I.; Nakamura, M.; Kuwano, H. *Sens. Actuators, B* **1996**, *37*, 163-168.

45. Edelman, P. G., Wang, J., Eds. *Acs Symposium Series: Biosensors and Chemical Sensors*; ACS: Washington DC, 1992.

46. Nakamura, R.; Muguruma, H.; Ikebukuro, K.; Sasaki, S.; Nagata, R.; Karube, I.; Pedersen, H. *Anal. Chem.* **1997**, *69*, 4649-4652.

47. Josowicz, M. *Analyst* **1995**, *120*, 1019-1024.

48. Lev, O.; Tsiousky, M.; Rabinovich, L.; Glezer, V.; Sampath, S.; Pankratov, I.; Gun, J. *Anal. Chem.* **1995**, *67*(1), 22A-30A.

49. Wang, J.; Pamidi, P. V. A. *Anal. Chem.* **1998**, *70*, 1171-1175.

50. Nakanishi, K.; Muguruma, H.; Karube, I. *Anal. Chem.* **1996**, *68*, 1695-1700.

51. Lev, O.; Wu, Z.; Bharathi, S.; Glezer, V.; Modestov, A.; Gun, J.; Rabinovich, L.; Sampath, S. *Chem. Mater.* **1997**, *9*, 2354-2375.

52. Dave, B. C.; Dunn, B.; Valentine, J. S.; Zink, J. I. *Anal. Chem.* **1994**, *66*(22), 1120A-1127A.

53. Chaiken, I.; Rose, S.; Karlsson, R. *Anal. Biochem.* **1992**, *210*, 197-210.

54. Lowe, C. R.; Dean, P. D. G. *Affinity Chromatography*; Wiley: London, 1974.

55. Turkova, J. *Affinity Chromatography*; Elsevier: Amsterdam, 1978.

56. Mohr, P.; Pommerening, K. *Affinity Chromatography*; Marcel Dekker Inc: New York, 1985.

57. Walters, R. R. *Anal. Chem.* **1985**, *57*(11), 1099A-1114A.

58. Tessema, M.; Csöregi, E.; Ruzgas, T.; Kenausis, G.; Solomon, T.; Gorton, L. *Anal. Chem.* **1997**, *69*, 4039-4044.

59. Masoom, M.; Townshend, A. *Anal. Chim. Acta* **1985**, *171*, 185-194.

60. Marko-Varga, G. A. *Anal. Chem.* **1989**, *61*, 831-838.

61. Matsumoto, K.; Baeza, J. J. B.; Mottola, H. A. *Anal. Chem.* **1993**, *65*, 1658-1661.

62. Zubritsky, E. *Anal. Chem. News & Features* **1999**, 172A.

63. Coterón, J. M.; Vicent, C.; Bosso, C.; Penadés, S. *J. Am. Chem. Soc.* **1993**, *115*, 10066-10076.

64. Eliseev, A. V.; Schneider, H. J. *J. Am. Chem. Soc.* **1994**, *116*, 6081-6088.

65. Das, G.; Hamilton, A. D. *J. Am. Chem. Soc.* **1994**, *116*, 11139-11140.

66. Scouten, W. H. Ed. *Solid Phase Biochemistry*; Wiley: New York, 1983.

67. Wulff, G. *Angew. Chem. Int. Ed. Engl.* **1995**, *34*, 1812-1832.

68. James, T. D.; Sandanayake, K. R. A. S.; Shinkai, S. *Angew. Chem. Int. Ed. Engl.* **1996**, *35*, 1910-1922.

69. Norrild, J. C.; Eggert, H. *J. Chem. Soc., Perkin Trans. 2* **1996**, *12*, 2583-2587.

70. Nollet, L. M. L., Ed. *Handbook of Food Analysis: Volume 2*; Marcel Dekker, Inc.: New York, 1996.

71. Whelan, W. J., Ed. *Biochemistry Series One Volume 5: Biochemitry of Carbohydrates*; Butterworths: London, 1975.

72. Valcárcel, M.; Luque de Castro, M. D. *Flow-Through (Bio)chemical Sensors*; Elsevier: Netherlands, 1994; pp 49-79.

73. Henry, C. *Anal. Chem. News & Features* **1996**, 625A-628A.

74. *Model QCA917 Quartz Crystal Analyzer Instruction Manual*; Seiko EG&G, 1994.

75. Bain, C. D.; Evall, J.; Whitesides, G. M. *J. Am. Chem. Soc.* **1989**, *111*, 7155-7164.

76. Elkins, E. R.; Matthys, A, Lyon, R.; Hunag, C. J. *J Food Composition & Analysis* **1996**, *9*, 43-56.

77. Braun, S.; Shtelzer, S.; Rappoport, S.; Avnir, D.; Ottolenghi, M. *J. Non-Cryst. Solids* **1992**, *147-148*, 739-743.

78. Brinker, C. J.; Scherer, G. W. *Sol-Gel Science: The Physics and Chemistry of Sol-Gel Processing*; Academic Press: Boston, 1990.

79. Aegerter, M. A.; Jafelicci, M.; Souza, D. F.; Zanotto, E. D. Eds. *Sol-Gel Science and Technology*; World Scientific: Singapore, 1989.

80. McDonagh, C.; Sheridan, F.; Butler, T.; MacCraith, B. D. *J. Non-Cryst. Solids* **1996**, *194*, 72-77.

81. Kraus, S. C.; Czolk, R.; Reichert, J.; Ache, H. J. *Sens. Actuators, B* **1993**, *15-16*, 199-202.

82. Zeigler, J. M.; Fearon, F. W. G. Eds. *Silicon-based Polymer Science: A Comprehensive Resource*; ACS: Washington D.C., 1990.

83. Sakka, S.; Kamiya, K. *J. Non-Cryst. Solids* **1982**, *48*, 31-46.

84. Mukkamala, R.; Cheung, H. M. *J. Mater. Sci.* **1997**, *32*, 4687-4692.

85. Jones, S. M.; Friberg, S. E.; Sjoblom, J. *J. Mater. Sci.* **1994**, *29*, 4075-4080.

86. Brinker, C. J.; Hurd, A. J.; Schunk, P. R.; Frye, G. C.; Ashley, C. S. *J. Non-Cryst. Solids* **1992**, *147-148*, 424-436.

87. Avnir, D.; Kaufman, V. R.; Reisfeld, R. *J. Non-Cryst. Solids* **1985**, *74*, 395-406.

88. Avnir, D.; Levy, D.; Reisfeld, R. *J. Phys. Chem.* **1984**, *88*, 5956-5959.

89. Avnir, D. *Acc. Chem. Res.* **1995**, *28*, 328-334.

90. Cho, G.; Moon, I. S.; Lee, J. S. *Chem. Lett.* **1997**, *6*, 577-578.

91. Pouchert, C. J. Ed. *The Aldrich Library of Infrared Spectra*; Aldrich Chemical Company: Wisconsin, 1981.

92. Nyquist, R. A.; Kagel, R. O. *Infrared Spectra of Inorganic Compounds*; Academic Press: New York, 1971.

93. Moulder, J. F.; Stickle, W. F.; Sobol, P. E.; Bomben, K. D. *Handbook of X-ray Photoelectron Spectroscopy*; Physical Electronics; New York, 1995.

94. Gomes, M.T.; Duarte, A. C.; Oliveira, J.P. *Anal. Chim. Acta* **1995**, *300*, 329-334.

Titles for Tables

Captions for Figures

Appendix I Typical applications of the QCA917 system

Principle		Application	
		Field	**Target**
Mass change		Gas sensing	Humidity Organic gas Odorant
		Immunoassay	Cells Micobes Biopolymers
	Visco-Elastic change	Electrochemical measurement	Ion sensing Electrochemical deposition Electrode reaction
		Thermal analysis	Phase transition analysis
Viscosity change		Gelation measurement	Endotoxin Blood coagulation factors
		Viscosity	Bioprocess

(From Ref. [73])

Appendix II QBASIC programs for data recording and calculations of rate constants

1. Program to record resonant frequency and admittance *vs.* time

```
DIM FR, TR, TI, TU
PRINT "Enter your frequency range(Hz):"
INPUT FR
PRINT "Enter the unit of TI and TR ( Hour 1, Minute 2, Second 3 )"
INPUT TU
PRINT "Enter your time range:"
INPUT TR
PRINT "Enter your time interval:"
INPUT TI

OPEN "C:\QCM\Freqval.001" FOR OUTPUT AS #2
WRITE #2, FR, TR, TI, TU                    'Save the parameter to the file

SCREEN 12                                   'Set the screen
DIM X0, Y0, XPLUS, YPLUS
WINDOW (0, 0) – (200, 200)
LINE (15, 30) – (15, 150), 4                'Draw Y axis
LINE (15, 90) – (115, 90), 4                'Draw X axis
X0 = 15                                     'Give X axis measuring unit
XPLUS = 5
DO UNTIL X0 > 117
    LINE (X0, 30) – (X0, 150), 8
    X0 = X0 + XPLUS
LOOP
Y0 = 30                                     'Give Y axis measuring unit
YPLUS = 5
DO UNTIL Y0 > 150
    LINE (15, Y0) – (115, Y0), 8
```

```
    Y0 = Y0 + YPLUS
LOOP
LINE (15, 90) – (115, 90), 7
LINE (65, 30) – (65, 150), 7

LOCATE 8, 3                          'Mark the unit of X axis with frequency value
PRINT FR
LOCATE 9, 3
PRINT "(Hz)"
LOCATE 17, 5
PRINT "0"
LOCATE 26, 3
PRINT –FR
LOCATE 18, 48
PRINT TR
LOCATE 19, 48
IF TU = 1 THEN
PRINT "(HOUR)"
END IF
IF TU = 2 THEN
PRINT "(MINUTE)"
END IF
IF TU = 3 THEN
PRINT "(SECOND)"
END IF

IF TU = 1 THEN                       'Set TU as second (conversion)
   TI = 3600 * TI
   TR = 3600 * TR
END IF
IF TU = 2 THEN
   TI = 60 * TI
   TR = 60 * TR
END IF
IF TU = 3 THEN
   TI = TI
   TR = TR
```

```
END IF

DIM Xunit, Yunit, X1, X2, Y1, Y2
DIM FREQ1#, FREQ2#, BEGIN, TEMP
Xunit = TI / TR * 100                                    'Mark X unit with time
X1 = 15
Y1 = 120
A1 = 80

DA = INT(TR / TI)
DIM FreqVal(1 To DA + 1), ADM(1 To DA + 1)    'Define array to save frequency
OPEN "COM2:9600, n, 8, 1, cs, ds" FOR RANDOM AS #1        'Set RS-232 port
PRINT #1, "RD 0"                                          'Read command
INPUT #1, FREQ1#, ADM1#
LOCATE 2, 3
PRINT "INITIAL (Hz) ="; : PRINT USING "#######.#"; FREQ1# / 10#;
PRINT ADM1#
TEMP = INT (FREQ1# / 1000000)
FREQ1# = FREQ1# - TEMP * 1000000
FreqVal (1) = FREQ1#
ADM (1) = ADM1#
I = 2
FREQ1# = FREQ1# / 10#
FOR J =1 TO DA
    BEGIN = TIMER
    DO WHILE TIMER < (BEGIN + TI)
  LOOP
    PRINT #1, "RD 0"
    INPUT #1, FREQ2#, ADM2#
    TEMP = INT(FREQ2# / 1000000)
    FREQ2# = FREQ2# - TEMP * 1000000
    FreqVal (I) = FREQ2#
    ADM (I) = ADM2#
    I = I + 1
    FREQ2# = FREQ2# / 10#
    Yunit = (FREQ2# - FREQ1#) /FR * 60
    Aunit = (ADM2# - ADM1#)
```

```
    LINE (X1, Y1) – (X1 + Xunit, Y1 + Yunit), 2
    LINE (X1, A1) – (X1 + Xunit, A1 + Aunit), 3
    X1 = X1 + Xunit
    Y1 = Y1 + Yunit
    A1 = A1 + Aunit
    FREQ1# = FREQ2#
    ADM1# = ADM2#
NEXT J
FREQ2# = TEMP * 1000000 + FREQ2# * 10#
LOCATE 4, 3
PRINT "LAST      (Hz) ="; : PRINT USING "#######.#"; FREQ2# / 10#;
PRINT ADM2#

WRITE #2, TEMP
FOR I = 1 TO DA
WRITE #2, FreqVal (I), ADM (I)
NEXT I                          'Save the array to the file (C:\QCM\FreqVal.001)

SHELL "GRAPHICS hpdefault"      'Load dos program to print graphics
pause = 5                       'Press (shift+PrintScreen) at this time
initial = TIMER
DO UNTIL TIMER > initial + pause
    TIMER ON
LOOP

END
```

2. Program for calculation of association rate constant

```
OPEN "C:\QCM\Freqval.001" FOR INPUT AS #1        'Input data
INPUT #1, FR, TR, TI, TU, TEMP                   'Input parameters

IF TU = 1 THEN                                   'Set TU as second (conversion)
    TI = 3600 * TI
    TR = 3600 * TR
```

```
END IF
IF TU = 2 THEN
    TI = 60 * TI
    TR = 60 * TR
END IF
IF TU = 3 THEN
    TI = TI
    TR = TR
END IF

DA + INT (TR / TI)
DIM FreqVal (1 TO DA + 1), ADM (1 TO DA + 1), DeltaF (1 TO DA)

FOR I = 1 TO DA
INPUT #1, FreqVal (I), ADM (I)                    'Input the first frequency value
FreqVal (I) = FreqVal (I) – INT (FreqVal (I) / 100000) * 100000
NEXT I

FOR J = 1 TO DA – 2
DeltaF (J) = (FreqVal (J) – FreqVal (J + 2)) * .5
NEXT J

OPEN "C\Kinetics\Ka\freqval.001" FOR OUTPUT AS #2
FOR J = 1 TO DA
WRITE #2, FreqVal (J + 1) / 10, DeltaF (J)
NEXT J

END
```

3. Program for calculation of dissociation rate constant

```
OPEN "C:\QCM\freqval.001" FOR INPUT AS #1          'Input data
INPUT #1, FR, TR, TI, TU, TEMP                     'Input parameters

IF TU = 1 THEN                                     'Set TU as second (conversion)
```

```
    TI = 3600 * TI
    TR = 3600 * TR
END IF
IF TU = 2 THEN
    TI = 60 * TI
    TR = 60 * TR
END IF
IF TU = 3 THEN
    TI = TI
    TR = TR
END IF

DA = INT (TR / TI)
DIM FreqVal (1 TO DA + 1), ADM (1 TO DA + 1), DeltaF (1 TO DA), TTIME (1
TO DA)
DB = 15

FOR I = 1 TO DA
INPUT #1, FreqVal (I), ADM (I)                    'Input the first frequency value
FreqVal (I) = FreqVal (I)
NEXT I

FOR J = 1 TO DA – DB –1
FreqVal (DB) = FreqVal (DB) – FreqVal (DA)
FreqVal (J + DB) = FreqVal (J + DB) – FreqVal (DA)
DeltaF (J) = LOG (FreqVal (DB) / FreqVal (J + DB))
TTIME (J) = .1 * J
NEXT J

OPEN "C:\Kinetics\Kd\freqval.001" FOR OUTPUT AS #2
FOR J + 1 TO dA
Write #2, TTIME (J), DeltaF (J)
Next J

END
```

Appendix III Response curves for different parameters obtained from numerical simulation

(From Reference [14])

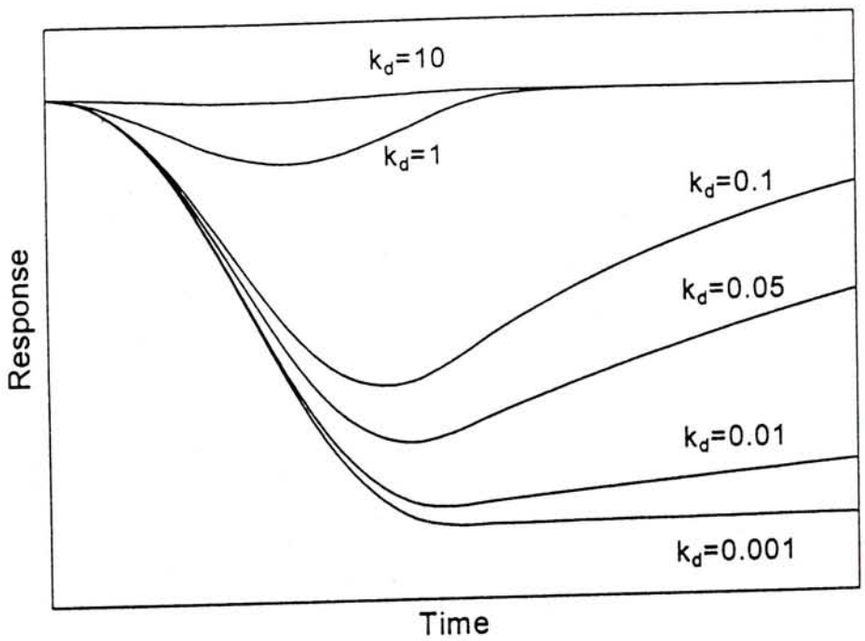

Figure III.1. Effect of k_d on the response curve with u=5, V_s=30, and $k_a C_b C_s$=1.

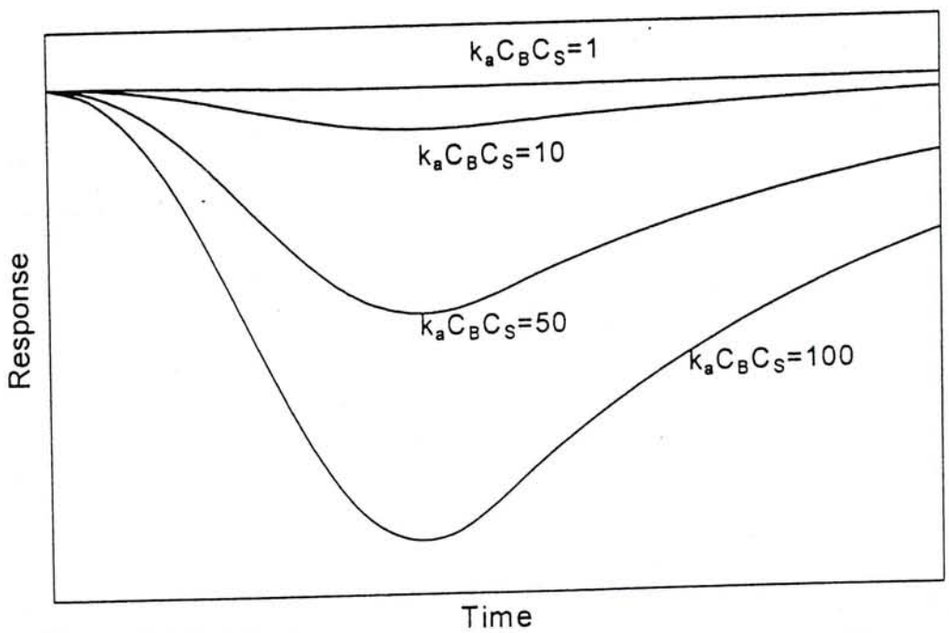

Figure III.2. Effect of $k_a C_b C_s$ on the response curve with u=5, V_s=30 and k_d=0.1.

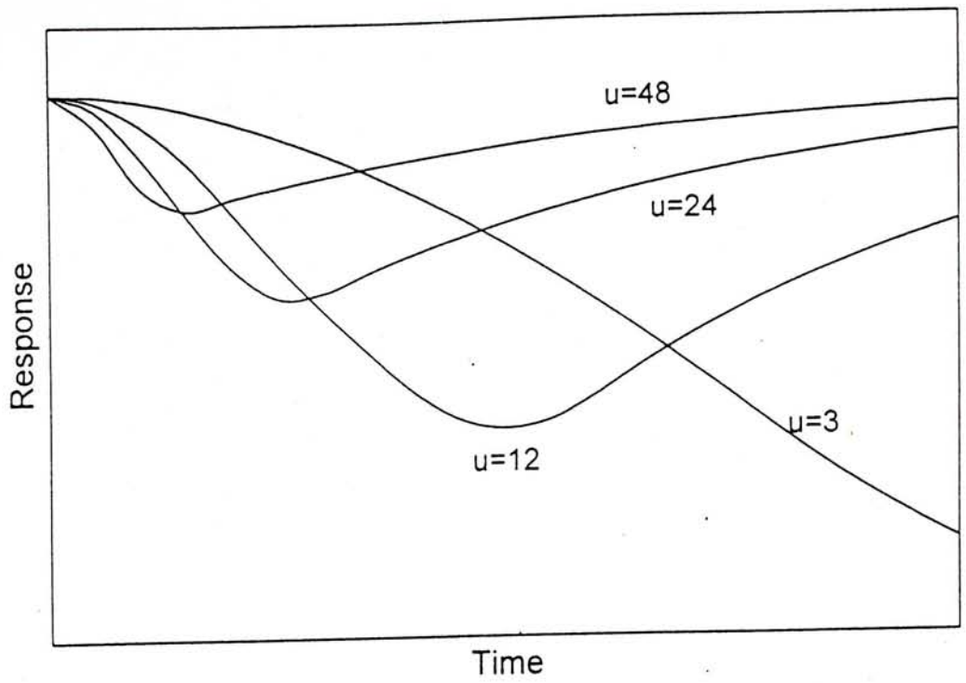

Figure III.3. Effect of flow velocity u on the response curve with V_s =30, $k_a C_b C_s$=1 and k_d=0.1.

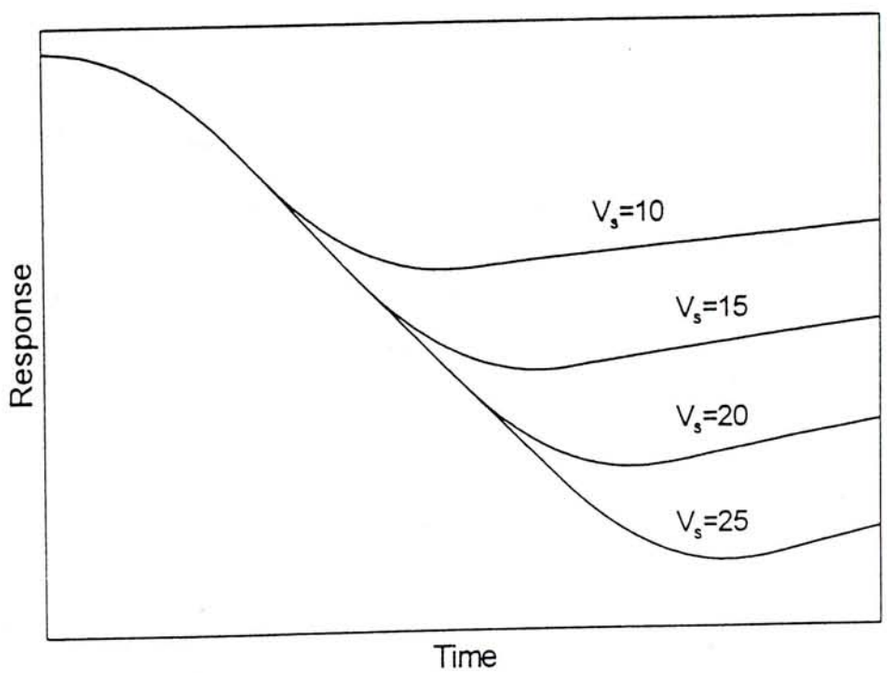

Figure III.4. Effect of the sample volume Vs on the response curve with u=10, $k_a C_b C_s$=1 and k_d=0.1.